1 # Processes controlling the seasonal variations of ^{210}Pb and

2 # ^{7}Be at the Mt. Cimone WMO-GAW global station, Italy: A

3 # model analysis

4 Erika Brattich[1], Hongyu Liu[2], Laura Tositti[1], David B. Considine[3], and James H.

5 Crawford[4]

6 [1] Department of Chemistry "G Ciamician", Alma Mater Studiorum University of

7 Bologna, Bologna (BO), 40126, Italy

8 [2] National Institute of Aerospace, Hampton, Virginia, Virginia, VA 23681, USA

9 [3] NASA Headquarters, Washington, DC 20546, USA

10 [4] NASA Langley Research Center, Hampton, Virginia, VA 23681, USA

11

12 **Correspondence to**: Hongyu Liu (hongyu.liu-1@nasa.gov)

13 **Abstract.** We apply the Global Modeling Initiative (GMI) chemistry and transport model

14 driven by the NASA's MERRA assimilated meteorological data to simulate the seasonal

15 variations of two radionuclide aerosol tracers (terrigenous ^{210}Pb and cosmogenic ^{7}Be) at the

16 WMO-GAW station of Mt. Cimone (44°12' N, 10°42' E, 2165 m asl, Italy), which is

17 representative of free-tropospheric conditions most of the year, during 2005 with an aim to

18 understand the roles of transport and precipitation scavenging processes in controlling their

19 seasonality. The total precipitation field in the MERRA data set is evaluated with the Global

20 Precipitation Climatology project (GPCP) observations, and a generally good agreement is

21 found. The model reproduces reasonably the observed seasonal pattern of ^{210}Pb concentrations,

22 characterized by a wintertime minimum due to lower ^{222}Rn emissions and weaker uplift from

Atmospheric
Chemistry
and Physics
Discussions

1 the boundary layer and summertime maxima resulting from strong convection over the

2 continent. The observed seasonal behavior of ^{7}Be concentrations shows a winter minimum, a

3 summer maximum, and a secondary spring maximum. The model captures the observed ^{7}Be

4 pattern in winter-spring, which is linked to the larger stratospheric influence during spring.

5 However, the model tends to underestimate the observed ^{7}Be concentrations in summer,

6 partially due to the sensitivity to spatial sampling in the model. Model sensitivity experiments

7 indicate a dominant role of precipitation scavenging (versus dry deposition and convection) in

8 controlling the seasonality of ^{210}Pb and ^{7}Be concentrations at Mt. Cimone.

9

10 **1 Introduction**

11   The use of atmospheric radionuclides to understand atmospheric dynamics, pollution

12 transport and removal processes has a long history (e.g., Junge, 1963; Reiter et al., 1971;

13 Gäggeler, 1995; Arimoto et al., 1999; Turekian and Graustein, 2003; WMO-GAW, 2004; Dibb,

14 2007; Rastogi and Sarin, 2008; Froehlich and Masarik, 2010; Lozano et al., 2012). It has been

15 recognized that natural radionuclides are useful in a global monitoring network for atmospheric

16 composition to support global climate change and air quality research, and therefore they are

17 measured at many of the regional, global and contributing-partner stations in the Global

18 Atmosphere Watch (GAW) network of the World Meteorological Organization (WMO)

19 (WMO-GAW, 2004). In particular, terrigenous ^{210}Pb and cosmogenic ^{7}Be natural radionuclides

20 are helpful in the understanding of the roles of transport and/or scavenging in controlling the

21 behaviors of radiatively active trace gases and aerosols (Balkanski et al., 1993; Koch et al.,

22 1996), as well as their anthropogenic (vs. natural) origin (e.g., Graustein and Turekian, 1996;

23 Arimoto et al., 1999; Liu et al., 2004; Cuevas et al., 2013). They are routinely monitored at

24 WMO-GAW stations around the world (Lee et al., 2004). Although ^{210}Pb and ^{7}Be have long

25 (1998-2011) been measured at the Global WMO-GAW station of Mt. Cimone (Italy), their

Atmospheric
Chemistry
and Physics
Discussions

1 seasonal behavior has not been thoroughly elucidated (Lee et al., 2007; Tositti et al., 2014).

2 Here we apply a state-of-the-art global chemistry and transport model (CTM) to the simulation

3 of ^{210}Pb and ^{7}Be, with an objective to better understand the roles of transport and precipitation

4 scavenging processes in controlling their seasonal variations at Mt. Cimone.

5   Because of their contrasting natural origins, ^{210}Pb and ^{7}Be have been used as a pair to

6 study the vertical transport and scavenging of aerosols (Koch et al., 1996). ^{210}Pb (half-life $\tau_{1/2}$

7 = 22.3 years) is the decay daughter of ^{222}Rn ($\tau_{1/2}$ = 3.8 days), which is emitted from soils by

8 decay of ^{226}Ra. The oceanic input of ^{222}Rn is about two orders of magnitude less than the

9 continental input and, because of the continental origin of ^{222}Rn, ^{210}Pb is considered as a tracer

10 of air masses with continental origin (Baskaran, 2011). ^{7}Be ($\tau_{1/2}$ = 53.3 days) is a cosmogenic

11 radionuclide generated by cosmic ray spallation reactions with nitrogen and oxygen (Lal et al.,

12 1958). Most (~67%) of ^{7}Be is produced in the stratosphere and the remaining (~33%) is

13 generated in the troposphere, particularly in the upper troposphere (Johnson and Viezee, 1981;

14 Usoskin and Kovaltsov, 2008). ^{7}Be is thus considered a tracer of stratospheric influence

15 (Viezee and Singh, 1980; Dibb et al., 1992, 1994; Liu et al., 2004, 2016) and subsidence (Feely

16 et al., 1989; Koch et al., 1996; Liu et al., 2004). Once produced, both radionuclides rapidly

17 attach onto aerosol particles in the fine fraction (Papastefanou and Ioannidou, 1995; Winkler

18 et al., 1998; Gaffney et al., 2004; Ioannidou et al., 2005), and are removed from the atmosphere

19 mainly by wet and secondarily dry deposition (Kulan et al., 2006). The concentrations of these

20 radionuclides in surface air thus depend on their sources, transport, wet and dry removal, and

21 radioactive decay (in the case of ^{7}Be). Rainfall scavenging processes are generally more

22 effective on ^{210}Pb than on ^{7}Be concentrations (Koch et al., 1996; Caillet et al., 2001; Likuku,

23 2006; Dueñas et al., 2009; Lozano et al., 2012).

Atmospheric
Chemistry
and Physics
Open Access
Discussions
EGU

1   Observational studies have previously been conducted to examine the factors influencing

2   surface ^{210}Pb and ^{7}Be concentrations in Europe, the Middle East and North Africa. Different

3   synoptic and mesoscale patterns are associated with the ranges of ^{210}Pb and ^{7}Be activity

4   concentrations (Lozano et al., 2012, 2013). In southwestern Spain (El Arenosillo), for instance,

5   low ^{210}Pb values are strongly linked to air masses from the Atlantic Ocean, whereas the highest

6   values are associated with air masses clearly under the influence of continents, such as the

7   Iberian Peninsula and North of Africa (Lozano et al., 2012). As for ^{7}Be, the highest ^{7}Be activity

8   concentrations over southwestern Iberian Peninsula are related with the arrival of air masses

9   from middle latitudes, and in particular from the Canary Islands, western Mediterranean Basin

10   and the north of Africa (Dueñas et al., 2011; Lozano et al., 2012).

11   With respect to ^{210}Pb and ^{7}Be spatial variability, ^{210}Pb concentrations in surface air are

12   strongly dependent on whether it is located over land or ocean, whereas ^{7}Be concentration is

13   mainly latitudinally dependent, due to their different production mechanisms. Generally

14   speaking, in the Northern Hemisphere higher ^{7}Be concentrations are present at middle latitudes

15   (20-50° N), because of the mixing of stratospheric air into the upper troposphere along the

16   tropopause discontinuity in mid-latitude regions and subsequent convective mixing within the

17   troposphere, which brings ^{7}Be-rich air masses into the planetary boundary layer and to the

18   earth's surface (Kulan et al., 2006). Lower ^{7}Be concentrations are towards the pole and towards

19   the equator (Kulan et al., 2006; Steinmann et al., 2013).

20   Many studies examined the seasonal behavior of ^{210}Pb and ^{7}Be at European mid-latitude

21   surface sites (e.g., Cannizzaro et al., 1999; Ioannidou et al., 2005; Daish et al., 2005; Todorovic

22   et al., 2005; Likuku, 2006; Dueñas et al., 2009; Pham et al., 2011; Carvalho et al., 2013;

23   Steinmann et al., 2013). High levels of ^{210}Pb during summer and low levels in winter were

24   found, reflecting the differing rates of ^{222}Rn emanation from soil above the European land mass

Atmospheric
Chemistry
and Physics
Discussions

Open Access

EGU

1   during winter (wet or snow covered soil) and summer (dry soil) (Hötzl and Winkler, 1987;

2   Caillet et al., 2001; Daish et al., 2005; Ioannidou et al., 2005). At low-elevation sites, monthly

3   ^{7}Be averages are characterized by a well-defined annual cycle with lower values during winter

4   and higher values during summer. Generally, the increase of ^{7}Be in ground level air from March

5   to May is ascribed to the more efficient and higher frequency stratosphere- troposphere

6   exchange (STE), whereas the further increase of ^{7}Be during summer is due to the stronger

7   convective mixing and higher tropopause (Ioannidou et al., 2014). The higher tropopause

8   height is associated with anticyclonic conditions, which results in downward transport from the

9   upper troposphere and reduced wet scavenging during these conditions (Gerasopoulos et al.,

10   2001, 2005; Ioannidou et al., 2014). In fact, compensating subsidence associated with

11   convective mixing enhances downward transport of ^{7}Be from the upper troposphere (rather

12   than direct input of stratospheric air) down to the lower troposphere and ground level (Zanis et

13   al., 1999; Gerasopoulos et al., 2001, 2005; Ioannidou et al., 2005; Likuku et al., 2006;

14   Steinmann et al., 2013).

15   High-elevation sites such as Jungfraujoch (Switerland), Zugspitze (Germany), and Mt.

16   Cimone (Italy), typically lying above the planetary boundary layer (PBL), are characterized by

17   lower ^{210}Pb concentrations and higher ^{7}Be due to direct influences of air masses from the free

18   troposphere (Zanis et al., 2000). The observed seasonal ^{210}Pb pattern at the high altitude sites

19   of Puy de Dome (1465 m asl, France) and Opme (660 m asl, France) is characterized by

20   maximum concentrations in spring and autumn and minimum concentrations in winter. This is

21   due to higher radon emissions during the dry season (summer) than during the wet season

22   (winter), and lower PBL height during winter (Bourcier et al., 2011). The latter results in

23   weaker upward transport of ^{222}Rn and ^{210}Pb at high-altitude sites. Similar to low-elevation sites,

24   higher ^{7}Be values are observed in summer due to convection-forced exchange with the upper

25   troposphere and to the higher tropopause height that leads to more efficient vertical transport

1   from the upper to lower troposphere (Reiter et al., 1983; Gerasopoulos et al., 2001; Bourcier et

2   al., 2011). At high-altitude sites a secondary maximum of [7]Be during cold months (December-

3   March) is generally observed and attributed to the increase in stratosphere-to-troposphere

4   events during this season (e.g., James et al., 2003; Stohl et al., 2003; Trickl et al., 2010). The

5   higher frequency of rapid subsidence in winter at Northern Hemisphere mid-latitudes can be

6   ascribed to the intensity of baroclinic systems, which is greatest in the wintertime. In fact, well-

7   developed tropopause folds and rapid deep intrusions are most likely to occur in the wake of

8   intense cyclogenesis, usually limited to the wintertime storm track regions (James et al., 2003).

9   Numerical models have been used to analyze ^{210}Pb and [7]Be observations at high-elevation

10   sites. 1-D model simulations of surface [7]Be showed higher concentrations at high-elevation

11   sites (Jasiulionis and Wershofen, 2005; Simon et al., 2009), but also suggested that the diffusion

12   of [7]Be was affected by the seasonal variation of meteorological conditions. Balkanski et al.

13   (1993) examined the transport of ^{210}Pb in a global 3-D model and reported a weak decrease of

14   ^{210}Pb concentrations between the continental mixed layer and the free troposphere: simulated

15   concentrations at 6-km altitude were about 50% of those in the continental mixed-layer over

16   much of the Northern Hemisphere in summer, and over large areas of the tropics year around,

17   a result consistent with the few observations available for the free troposphere at that time

18   (Moore et al., 1973). Rehfeld and Heimann (1995) compared the 3-D model simulated seasonal

19   pattern of surface ^{210}Pb and [7]Be concentrations with the observations at several sites in both

20   hemispheres. At Mauna Loa (19.47°N, 155.6°W, 3400 m asl, Hawaii) ^{210}Pb seasonality was

21   characterized by high concentrations in spring and summer and lower ones in winter, as

22   opposed to the seasonal pattern found at higher latitudes, where the ^{210}Pb maximum

23   concentrations in winter are attributed to the advective transport of ^{210}Pb aerosols from mid-

24   latitudes. This behavior is due to the elevation of the site, representative of the conditions of

25   the free troposphere rather than those of the PBL. As for [7]Be, the comparison between the

1 model and the observations at Rexburg (43.8°N, 111.83°W, 1483 m asl, USA) showed

2 systematically lower model values, due to the much higher precipitation rates in the model.

3 Previous studies have examined surface ^{7}Be observations at Mt. Cimone with respect to

4 the role of STE in surface ozone increases (Bonasoni et al., 1999, 2000ab; Cristofanelli et al.,

5 2003, 2006, 2009a, 2015; Lee et al., 2007) within the framework of European projects such as

6 VOTALP (Vertical Ozone Transport in the Alps) and STACCATO (influence of Stratosphere-

7 Troposphere exchange in A Changing Climate on Atmospheric Transport and Oxidation

8 capacity). These studies led to the assessment of a higher incidence of STE events during the

9 period from October to February relative to the warm season, when thermal convection and the

10 rising of the tropopause promote vertical mixing, which acts as a confounding factor in STE

11 detection. Lee et al. (2007) and Tositti et al. (2014) reported the seasonal patterns and frequency

12 distributions of ^{210}Pb and ^{7}Be measured at Mt. Cimone, and highlighted higher concentrations

13 of both radionuclides in the summertime due to the higher mixing height and horizontal

14 transport by regional airflows. During winter, a general increase in ^{7}Be is associated with a

15 decrease in ^{210}Pb, due to the dominating effect of STE and subsidence in the free troposphere.

16 At the time of this work, no model analyses of ^{210}Pb and ^{7}Be observations at the site have been

17 conducted.

18 In this paper, we conduct simulations of ^{210}Pb and ^{7}Be at Mt. Cimone with a state-of- the-

19 art global 3-D chemistry and transport model (GMI CTM) driven by assimilated

20 meteorological fields for the year of 2005. Our objectives are a better elucidation of the

21 seasonal variations of ^{210}Pb and ^{7}Be concentrations and an improved understanding of the roles

22 of transport and precipitation scavenging processes in their seasonalities at Mt. Cimone.

23 The remainder of this paper is organized as follows. Section 2 describes the measurement

24 site, the radioactivity measurements at Mt. Cimone, and the GMI CTM. Section 3 evaluates

7

Atmospheric
Chemistry
and Physics
Discussions

1   the model performance in reproducing the observed wind and precipitation fields. Section 4

2   evaluates the seasonal ^{210}Pb and ^{7}Be concentrations in the model with those observed. Section

3   5 examines the sources and seasonal variations in the simulated radionuclide activities,

4   followed by summary and conclusions in section 6.

5   **2 Data and Methods**

6   **2.1 Radionuclide Measurements at Mt. Cimone**

7   Mt. Cimone station (44°12' N, 10°42' E, 2165 m asl) is a global WMO-GAW station

8   managed by the Meteorological Office of the Italian Air Force, which hosts the research

9   platform "Ottavio Vittori" of the Institute of Atmospheric and Climate Science of the National

10   Council of Research (ISAC-CNR). The station is located on top of the highest peak of the

11   Italian northern Apennines, with a 360° free horizon and an elevation such that the station lies

12   above the PBL during most of the year: the Mt. Cimone measurements are considered

13   representative of the southern Europe/Mediterranean free troposphere (Bonasoni et al., 2000a;

14   Fischer et al., 2003; Cristofanelli et al., 2007), although during the warmer months an influence

15   of PBL air can be detected due both to convective processes and mountain/valley breeze

16   regimes (Fischer et al., 2003; van Dingenen et al., 2005; Tositti et al., 2013). Note in this

17   framework that southern Europe and Mediterranean basin are considered as a hot-spot region

18   in terms of both climate change (e.g., Forster et al., 2007) and air quality (Monks et al., 2009),

19   as well as a major crossroad of different air mass transport processes (Li et al., 2001; Lelieveld

20   et al., 2002; Millàn et al., 2006; Duncan et al., 2008; Tositti et al., 2013).

21   At Mt. Cimone station, ^{210}Pb, ^{7}Be, and aerosol mass load in the form of PM$_{10}$ have been

22   regularly measured in the period of 1998-2011 with a Thermo-Environmental PM$_{10}$ high-

23   volume sampler. PM$_{10}$ is sampled on rectangular glass fiber filters (Whatman, 20.3 cm × 25.4

24   cm, with an effective exposure area of about 407 cm^{2}), which were manually changed every 2-

1   3 days, depending on weather conditions, failures of the sampling equipment and/or of the

2   power supply and personnel on site. The average flow rate was about 1.13 m^3 min^{-1} at standard

3   temperature and pressure (STP), with an average volume of air collected on each filter equal

4   to 3000-4000 m^3 (about 48 hours of sampling, 115-175 samples per year).

5   Airborne radionuclides travel attached to particulate matters, and as a consequence of

6   their physical origin, tend to populate the fine fraction (<1.0 μm) (Winkler et al., 1998; Gaffney

7   et al., 2004). The PM_{10} samples were subjected to non-destructive high-resolution γ-

8   spectrometry for the determination of airborne radiotracers ^{210}Pb and ^{7}Be. The characteristics

9   of the two Hyper Pure Germanium crystal detectors (HPGe) detectors are as follows: one p-

10   type coaxial detector by Ortec/Ametek with a relative efficiency of 32.5% and FWHM 1.8 keV

11   at 1332 keV and one planar DSG detector with an active surface of 1500 mm^2 and FWHM 0.73

12   keV at 122 keV, for higher and lower energy ranges (100-2000 keV and 0-900 keV),

13   respectively.

14   Spectra were accumulated for at least one day to optimize peak analysis and then

15   processed with a specific software package (GammaVision-32, version 6.07, Ortec). Efficiency

16   calibration was determined on both detectors with a blank glass fiber filter traced with

17   accurately weighted aliquots of a standard solution of mixed radionuclides (QCY48,

18   Amersham) supplemented with ^{210}Pb, homogeneously dispersed dropwise over the filter

19   surface. Once dried under a hood under ambient conditions, the calibration filter was folded

20   into a polystyrene container in the same geometry as the unknown samples. Quantitative

21   analysis on samples was carried out by subtracting the spectrum of a blank filter in the same

22   geometry, while uncertainty on peaks (k = 1, 68% level of confidence) was calculated

23   propagating the combined error over the efficiency fit previously determined with the counting

24   error. Minimum detectable activity was calculated making use of the traditional ORTEC

25   method (ORTEC, 2003) with a peak cut-off limit of 40%. Activity data was corrected to the

1   midpoint of the time interval of collection and for the decay during spectrum acquisition. For

2   our analysis, we used monthly averages of ^{210}Pb and ^{7}Be data at Mt. Cimone in 2005.

3   **2.2 GMI Model**

4   The Global Modeling Initiative (GMI, http://gmi.gsfc.nasa.gov) is a NASA-funded

5   project aiming at improving assessments of anthropogenic perturbations to the Earth system;

6   in this framework a CTM appropriate for stratospheric assessments was developed (Rotman et

7   al., 2001). It was firstly used to evaluate the potential effects of stratospheric aircraft on the

8   global stratosphere (Kinnison et al., 2001) and on the Antarctic lower stratosphere (Considine

9   et al., 2000). The recent version of the GMI CTM includes a full treatment of both stratospheric

10 and tropospheric photochemical and physical processes and is also capable of simulating

11 atmospheric radionuclides ^{222}Rn, ^{210}Pb, ^{7}Be, and ^{10}Be throughout the troposphere and

12 stratosphere (Considine et al., 2004, 2005; Rodriguez et al., 2004; Liu et al., 2016). Details of

13 the model are described in Duncan et al. (2007, 2008), Strahan et al. (2007), and Considine et

14 al. (2008).

15 In this work a version of the GMI model with the same basic structure as described by

16 Considine et al. (2005) and Liu et al. (2016) was used, including parameterizations of the

17 important tropospheric physical processes such as convection, wet scavenging, dry deposition

18 and planetary boundary layer mixing. Meteorological data used to drive the CTM, e.g.,

19 horizontal winds, convective mass fluxes and precipitation fields, are the Modern-Era

20 Retrospective analysis for Research and Applications (MERRA) assimilated data set from the

21 NASA Global Modeling and Assimilation Office (GMAO) (Rienecker et al., 2011).

22 The flux-form semi-Lagrangian advection scheme and a convective transport algorithm

23 from the CONVTRAN routine in NCAR CCM3 physics package are used in the model. The

24 wet deposition scheme is that of Liu et al. (2001): it includes scavenging in wet convective

25 updrafts, and first-order rainout and washout from both convective anvils and large-scale

Atmospheric
Chemistry
and Physics
Discussions
Open Access
EGU

1 precipitations. The gravitational settling effect of cloud ice particles included in Liu et al.

2 (2001) is not considered here. Dry deposition of aerosols is computed using the resistance-in-

3 series approach. For the simulations of radionuclides, each simulation was run for six years,

4 recycling the meteorological data for each year of the simulation, to equilibrate the lower

5 stratosphere as well as the troposphere (Liu et al., 2001). The sixth year output was used for

6 analysis.

7   A uniform ^{222}Rn emission of 1.0 atom cm^{-2} s^{-1} from land under nonfreezing conditions is

8 assumed (Liu et al., 2001). Following Jacob and Prather (1990), the flux is reduced by a factor

9 of 3 under freezing conditions. The flux from oceans and ice is null. Although a large variability

10 of ^{222}Rn emission from land is observed, the above emission estimate is thought to be accurate

11 to within 25% globally (Turekian et al., 1977) and to within a factor of 2 regionally (Wilkening

12 et al., 1975; Schery et al., 1989; Graustein and Turekian, 1990; Nazaroff, 1992; Liu et al.,

13 2001).

14   Following Brost et al. (1991) and Koch et al. (1996), we used the Lal and Peters (1967)

15 ^{7}Be source for 1958 (solar maximum year), as it best simulated stratospheric ^{7}Be concentrations

16 measured from aircraft (Liu et al., 2001). No interannual variability in the ^{7}Be source is

17 considered in the model (Liu et al., 2001). This may lead to an underestimate of tropospheric

18 ^{7}Be concentrations, especially at high latitudes during a solar minimum (or near minimum)

19 year. Lal and Peters (1967) reported that the relative amplitude of the ^{7}Be production rate over

20 a 11-year solar cycle is about 13% below 300 hPa at latitudes above 45 degree.

21   Because of the coarse horizontal resolution of the model (2° latitude by 2.5° longitude),

22 the model representation of the topography at the site is poor. The elevation of Mt. Cimone in

23 the model is only 298 m, whereas in reality the mountain is 2165 m (asl) high (Figure 1). For

24 this reason, the model output was not sampled at ground level, but at the gridbox corresponding

25 to the elevation of the site. In order to see the sensitivity of model-observation comparisons to

Atmospheric
Chemistry
and Physics
Discussions

1   spatial sampling, the model was sampled not only for the grid corresponding to the latitude and

2   longitude of Mt. Cimone, but also for the 8 adjacent grids. To better understand the sources

3   and seasonality of radiotracers in the model, we examine model output not only for ^{210}Pb, ^{7}Be

4   and their ratio ^{7}Be/^{210}Pb (an indicator of vertical transport [Koch et al., 1996]), which can be

5   directly compared to the measurements taken at Mt. Cimone, but also for other radiotracers and

6   quantities, e.g., ^{222}Rn, and ^{10}Be/^{7}Be (a STE tracer [Zanis et al., 2003]).

7   Year 2005 was chosen for analysis because of the availability of the observational data

8   and model output at the time of this work. As discussed later, the seasonal behavior of ^{210}Pb

9   and ^{7}Be radionuclides during year 2005 was "typical" for Mt. Cimone. Monthly averages of

10   ^{210}Pb and ^{7}Be data at Mt. Cimone were calculated for comparison with model results. To better

11   compare the seasonalities of ^{210}Pb and ^{7}Be between the model and the observations, the

12   monthly percentage deviations from the annual mean concentration were also calculated.

13   **3 Seasonal Variations of Transport and Precipitation at Mt. Cimone: Observations vs.**

14   **Model Simulations**

15   Mt. Cimone is the windiest meteorological station in Italy and the prevailing local winds

16   blow from S-SW and N-NE directions (Ciattaglia, 1983; Ciattaglia et al., 1987; Colombo et al.,

17   2000). The wind observations at Mt. Cimone during the period of 1998-2011, when

18   radionuclide measurements were performed at the station (Tositti et al., 2014), agree with the

19   climatology of local wind intensity and direction during the period of 1946-1999 as reported

20   by the Italian Air Force (Colombo et al., 2000). N-NE directions are more significant during

21   the cold period, and fluxes from SW are more typical of the warm period. While winds blowing

22   from the S-SW sector generate a sea air inflow, a continental air inflow is observed when winds

23   come from the N-NE sector (Ciattaglia et al., 1987).

24   However, when considering the lifetimes of ^{210}Pb (about one week) and ^{7}Be (about three

25   weeks) aerosols (Liu et al., 2001), it is apparent that the regional and long-range transport has

1   a much more important role than local transport. On a large scale, about 70% of background

2   air masses reaching Mt. Cimone in the period of 1996-1998 came from Atlantic and Arctic

3   areas, with a smaller contribution from the Mediterranean Basin and the eastern area, as

4   estimated by Bonasoni et al. (2000). A more recent and extended study of advection patterns

5   at Mt. Cimone (Brattich E. et al., "Advection patterns at the WMO-GAW station of Mt.

6   Cimone: seasonality, trends, and influence on atmospheric composition", manuscript in

7   preparation, 2016), analyzing clusters of 4-day kinematic back-trajectories calculated for the

8   period of 1998-2011 with the HYSPLIT (HYbrid Single-Particle Lagrangian Integrated

9   Trajectory) model driven by the NCEP/NCAR (National Center for Environmental

10   Prediction/National Center for Atmospheric Research) meteorological reanalysis, shows that

11   the air masses advected to Mt. Cimone (55%) arrive from the Western-Atlantic-North America

12   sector, while the remaining air masses (from the Arctic, Eastern and Mediterranean Basin-

13   Northern Africa) together represent 45% of trajectories. Seasonal transport to Mt. Cimone in

14   the model is shown in Figure 2, representing winds at the elevation of Mt. Cimone (winds are

15   weaker at the model bottom layer). In agreement with the description of advection patterns at

16   the site, prevailing model winds (Figure 2) blow from the western-Atlantic sector. Slow

17   summer winds suggest the stronger influence of regional/local transport at Mt. Cimone during

18   the period (e.g., Lee et al., 2007; Marinoni et al., 2008; Tositti et al., 2013, 2014; Brattich et

19   al., 2015).

20   In the model Mt. Cimone appears to be in a location where there is a large horizontal

21   gradient of wind (transport). Long-range transport from Western Europe, North America and

22   Arctic region prevail during the cold period, while regional transport appears more important

23   in summer. The model is able to capture relevant features of pressure systems and seasonal

24   circulation patterns of the North Atlantic/Mediterranean/African region, such as the semi-

25   permanent high pressure system located in the North Atlantic with different positions during

Atmospheric
Chemistry
and Physics
Discussions

Open Access

EGU

1 different seasons (Bermuda/Azores high), a semi-permanent system of high pressure centered

2 in northeastern Siberia during the colder half of the year (Siberian high), and the ITCZ in the

3 summer/autumn season. However, due to the coarse resolution of the global meteorological

4 reanalysis that we use to construct the model winds, the more than 50 local-scale wind systems

5 present in the Mediterranean and surrounding regions are not resolved (Burlando, 2009). In

6 northern Europe, in fact, there are approximately two main states for the atmosphere, the

7 westerly or zonal flows modulated by the advection of Atlantic lows, and the long-lived

8 blocking anticyclonic configurations over North Sea or Scandinavia (easterly) (Burlando et al.,

9 2008).

10 In the Mediterranean region, the main cyclones during winter are essentially sub-synoptic

11 lows triggered by the major North-Atlantic synoptic systems affected by the local topography

12 of the Northern Mediterranean coast (Trigo et al., 2002), whereas in summer cyclones develop

13 because of thermal effects, orography (e.g., the Atlas Mountains), and increase in low-level

14 thermal gradients (Trigo et al., 2002; Campins et al., 2006). Again, due to the coarse resolution

15 of the meteorological data we use, these sub-synoptic processes are not resolved. For instance,

16 North-African lows and Sahara depressions (also referred to as Atlas lee depressions) and the

17 resulting S-SW wind (Sirocco) (Reiter, 1975), potentially linked to ^{210}Pb variations at Mt.

18 Cimone, appear to be an important feature missing in the degraded MERRA data, where they

19 appear only during October/November.

20 We evaluate the MERRA precipitation with those from the GPCP (Global Precipitation

21 Climatology Project, http://www.gewex.org/gpcp.html) satellite and surface observations in

22 2005. Figure 3 shows the MERRA and GPCP monthly precipitation for the region defined by

23 0-75°N and 90°W – 90°E. A good agreement between the MERRA and the GPCP

24 precipitations averaged over the region was found. In particular, summer precipitation patterns

25 are very similar. The geographical distribution of precipitation in MERRA shows some

1 important features in agreement with the observed climatology precipitations: the desert

2 climate in North Africa with very low precipitation all year long, the ITCZ with high

3 precipitation during the summer/autumn seasons, the North Atlantic region with high

4 precipitation especially during the winter and autumn seasons, and Europe where the seasonal

5 pattern of precipitation is similar to that in the North Atlantic region, but precipitation is lower.

6   Figure 4 shows the comparison of the GPCP and MERRA precipitation seasonality at Mt.

7 Cimone. Since Mt. Cimone is located in a region with a large horizontal gradient in

8 precipitation, we also show in the figure the comparisons for three adjacent gridboxes. The

9 agreement between the MERRA and GPCP precipitation seasonality is reasonable, with the

10 squared correlation coefficient R^2 varying between 0.56 (at the grid to the northwest of "ij")

11 and 0.89 (at the grid to the southeast of "ij"). Large differences between the MERRA

12 precipitation and that locally observed at the station are instead present (not shown): in

13 particular, the MERRA precipitation is larger during winter-autumn, while it is much more

14 similar to that observed during spring-summer. This difference may very well reflect again the

15 fact that the observed surface precipitation is localized, whereas the satellite and MERRA

16 precipitations correspond to a much larger scale (about 200 km). Moreover, as Colombo et al.

17 (2000) previously pointed out, different from the surrounding area where the climate is defined

18 as temperate-continental, the climate at the mountaintop is classified as alpine because of the

19 high elevation. In fact, in agreement with the GPCP precipitation in 2005, the observed

20 climatology in the region shows maximum during November (secondary maximum in spring)

21 and absolute minimum in July (secondary minimum in January), whereas on the top of the

22 mountain the precipitation is maximal during summer. The MERRA precipitation shows

23 increased amounts during April and August-December, with minimum in June-July. As the

24 local precipitation at the site is important to the scavenging of radionuclide aerosol tracers, this

25 difference between the local and regional precipitation could contribute to any biases in our

Atmospheric
Chemistry
and Physics
Discussions

1   simulations. However, as we will show below, the ratio $^{7}Be/^{210}Pb$ may cancel out the errors

2   associated to precipitation scavenging (Koch et al., 1996).

3   Low ^{210}Pb concentrations are seen over the Atlantic Ocean, due to the negligible

4   emissions of ^{222}Rn from the oceans and strong precipitation scavenging, and in northern and

5   western Europe especially during the cold season (Figure 2a). High ^{210}Pb concentrations appear

6   over the Sahara desert and North Africa, as a result of low precipitation in this area, and also

7   over the Middle East and South Asia. ^{210}Pb concentrations over southern Europe appear higher

8   during the transition seasons, especially fall, and peak during summer when the minimum

9   precipitation and slow winds from west are observed in the region. Low ^{7}Be concentrations are

10 simulated along the equator where convective scavenging is strongest (Figure 2b). High ^{7}Be

11 concentrations are seen over the Sahara desert due to a combination of low precipitation and

12 subsidence in this region. Elevated values also occur over the Middle East, North America, and

13 Greenland. ^{7}Be concentrations over southern Europe appear higher during spring and peak

14 during winter, when model winds are stronger and transport ^{7}Be aerosols from North America

15 and Greenland regions where ^{7}Be production is highest (Beer et al., 2012).

16 **4 Seasonal Variations of ^{210}Pb and ^{7}Be at Mt. Cimone: Observations vs. Model**

17 **Simulations**

18   The seasonality and frequency distributions of ^{210}Pb and ^{7}Be concentrations measured at

19 the Mt. Cimone station were previously examined by Lee et al. (2007), while more recent

20 analyses of the 12-year record were presented in Tositti et al. (2014) and Brattich et al. (2015).

21 Generally, both radionuclides show a marked seasonal maximum in the summertime, a

22 behaviour shared by PM_{10} (Tositti et al., 2013) and O_3 (Bonasoni et al., 2000b). ^{210}Pb summer

23 maximum is mainly due to the higher mixing height and enhanced uplift from the boundary

24 layer as a result of thermal convection. The seasonal fluctuation of ^{7}Be is more complex and

25 characterized by two relative maxima, one during the cold season associated with stratosphere-

Atmospheric
Chemistry
and Physics
Discussions

1   to-troposphere transport, and the other during the warm season mainly associated with

2   tropospheric subsidence balancing lower-tropospheric air masses ascent occasionally

3   accompanied by STE (Tositti et al., 2014). The ^{210}Pb and ^{7}Be measurements in 2005 are

4   consistent with this description (Figure 5): ^{210}Pb concentrations are characterized by two

5   maxima during the warm period (July and September); ^{7}Be concentrations are characterized by

6   one absolute maximum during summer (July) and one secondary maximum during spring

7   (March).

8   Figure 5 (ab) compares the simulated monthly ^{210}Pb and ^{7}Be activities with the

9   observations at Mt. Cimone in 2005. The comparisons for the monthly percentage deviations

10   from the annual mean concentration are available as Supplementary Information (hereafter SI,

11   SI Figures 1-2). The seasonality of ^{210}Pb is well captured by the model. The model reproduces

12   the presence of two seasonal maxima in the ^{210}Pb observations, with the maximum observed in

13   July shifted to June in the simulation. The squared correlation coefficient R^2 between observed

14   and simulated ^{210}Pb activities is equal to 0.83 at the "ij" grid and varies between 0.42 and 0.82

15   for adjacent gridboxes (to the north and to the west of "ij", respectively), confirming the good

16   performance of the model in reproducing the ^{210}Pb seasonal pattern.

17   As for ^{7}Be, the model well captures the March maximum (i.e., secondary maximum in

18   the observations) and the general seasonal pattern during the cold and transition seasons.

19   However, during the warm period, the simulated ^{7}Be concentrations are lower by a factor of 2

20   than the observed. A better agreement was found at some adjacent model gridboxes (e.g., "to

21   the south and to the southwest of "ij"; Figure 6 vs. Figure 5). The correlation between observed

22   and simulated monthly ^{7}Be activities also increases from $R^2 = 0.03$ at "ij" to $R^2 = 0.11\text{-}0.60$ at

23   adjacent model gridboxes.

24   **5 Sources and Seasonality of ^{210}Pb and ^{7}Be at Mt. Cimone: A Model Analysis**

17

Atmospheric
Chemistry
and Physics
Discussions

1   In this section, we quantify the sources of ^{210}Pb and ^{7}Be and determine the processes

2   governing their seasonality in the GMI model. Additional tracers as simulated by the model are

3   used to aid in the interpretation. Model sensitivity experiments are conducted to examine the

4   roles of transport and precipitation scavenging in the seasonality.

5   As discussed in Section 4, the model well reproduces the ^{210}Pb seasonality, with

6   minimum in the cold period and maximum in the warm period. The ^{210}Pb seasonality (Figure

7   5a) can be linked with the seasonal pattern of its precursor ^{222}Rn (Figure 5c). It is seen that the

8   summer ^{210}Pb maximum is due to stronger (thermal) convection, which uplifts more ^{222}Rn out

9   of the boundary layer (e.g., Lee et al., 2007; Tositti et al., 2014; Brattich et al., 2015). This

10   uplift of ^{222}Rn from the boundary layer is minimum in the cold period, and the minimal level

11   of ^{210}Pb in this period can be considered representative of the free troposphere. The ^{210}Pb

12   summer increase appears to be associated with short-range and regional transport, as suggested

13   by the model simulations (Figure 2a). As expected, long-range transport is more typical of the

14   winter/spring seasons because of stronger horizontal winds, while regional effects are more

15   important during summer when convection gets stronger.

16   In a similar manner, the source of the ^{7}Be March maximum can be investigated with

17   model tracer simulations. Figure 5 (de) also shows the simulated seasonal patterns of the

18   ^{10}Be/^{7}Be activity ratio and of the fraction of ^{7}Be originating from the stratosphere (strat

19   ^{7}Be/total ^{7}Be). The simulated seasonal pattern of the ^{10}Be/^{7}Be ratio is very similar to the

20   observations at Zugspitze (Germany, 2962 m asl) (Zanis et al., 2003), characterized by a not-

21   pronounced seasonal cycle with somewhat elevated ratios in February-April and June-July.

22   The usefulness of ^{10}Be/^{7}Be ratio as a stratospheric tracer is due to the fact that both ^{10}Be and

23   ^{7}Be cosmogenic radionuclides attach to the same aerosols and share therefore the same removal

24   mechanism. Moreover, due to the much longer physical half-life of ^{10}Be ($\tau_{1/2} = 1.5 \times 10^6$ years)

25   compared to ^{7}Be ($\tau_{1/2} = 53.3$ days), their concentration ratios in the stratosphere (about 3-4) are

Atmospheric
Chemistry
and Physics
Discussions

1   much higher than in the troposphere (about 2 or even less) (Koch and Rind, 1998). The

2   simulated ^{10}Be/^{7}Be ratio behavior indicates that deep stratosphere-to-troposphere (STT) peaks

3   during winter, while shallower STT has a spring maximum, consistent with previous analyses

4   of stratospheric intrusions at Mt. Cimone (Cristofanelli et al., 2006, 2009), and more generally

5   with the climatology of stratosphere-troposphere exchange at the Northern Hemisphere mid-

6   latitudes (James et al., 2003). Altogether the simulated high strat ^{7}Be/total ^{7}Be, high ^{7}Be/^{210}Pb

7   (Figure 7), and low ^{10}Be/^{7}Be ratios during December-January indicate strongest STE during

8   this period, followed by spring with slightly weaker stratospheric influence on surface ^{7}Be.

9   However, the model tends to overestimate the observed ^{7}Be concentrations and ^{7}Be/^{210}Pb ratios

10   during December-February, suggesting that STE and/or subsidence in the model is likely too

11   fast in this region. As reported by Huang et al. (2013), a stronger net subsidence of air masses

12   to the surface could be due to unrealistic meteorological conditions (e.g., boundary layer

13   structure, wind fields, vertical mixing).

14   The use of the ^{7}Be production rate of Lal and Peters (1967) for a solar maximum year

15   (1958) may partly explain the lower annual mean ^{7}Be in the model (3.4 mBq m^{-3} annual mean

16   at the "ij" grid) than in the observations (4.2 mBq m^{-3}). In fact, the sunspot number in 2005

17   (29.8) was quite low (slowly decreasing from 2000, a solar maximum year, and reaching

18   minimum in 2008), especially compared to the 1958 value of 184.8. Sunspot number data are

19   available from the World Data Center for the production, preservation and dissemination of the

20   international sunspot number (Sunspot Index and Long-term Solar Observation, SILSO, Royal

21   Observatory of Belgium, Brussels, http://sidc.oma.be/sunspot-data/).

22   During the winter period, associated with the simulated and observed ^{7}Be increases

23   (Figures 5-6), strong long-range transport was dominant in the European region (Figure 2b).

24   Transport from higher latitude regions (Arctic, northern Europe, and North America) appears

25   particularly important during this period (Figure 2b); such transport from high-latitude regions,

Atmospheric
Chemistry
and Physics
Discussions

Open Access

EGU

1   where the ^{7}Be production rate is highest (Beer et al., 2012), has typically been observed during

2   STE events at Mt. Cimone in many studies (e.g., Bonasoni et al., 1999, 2000ab).

3   The discrepancy between the simulated and the observed ^{7}Be concentrations during the

4   warm period is partly due to the sensitivity to spatial sampling in the model. As seen from the

5   map plots of ^{210}Pb and ^{7}Be concentrations at the elevation of Mt. Cimone (Figure 2), the

6   sampling site appears to be located in a region where the N-S gradient of concentrations is large

7   (especially for ^{7}Be). An elevated gradient in the region surrounding Mt. Cimone was also seen

8   for winds, as transport plays a critical role in determining the distributions of these tracers. The

9   sensitivity to spatial sampling in the model is therefore ascribed to this observed strong gradient

10   in the N-S direction. In fact, while the grids to the south and southwest of "ij" are better for

11   summer ^{7}Be comparisons (Figure 6), the grids to the northeast, north, and northwest of "ij" are

12   better for winter (not shown).

13   The model underestimate of ^{7}Be levels in the warm months may also suggest the mixing

14   of air masses between the PBL and the lower free troposphere is likely too weak. Previous

15   observational analyses indicated that such mixing is higher in summer at Mt. Cimone due to

16   enhanced convection and mountain wind breeze (e.g., Fischer et al., 2003; Cristofanelli et al.,

17   2007). Weaker entrainment of free-tropospheric air into the PBL would result in lower ^{7}Be

18   concentrations at the surface.

19   The model annual average biases are about 8% for ^{210}Pb and about 19% for ^{7}Be,

20   respectively. By contrast, the model average bias for ^{7}Be/^{210}Pb ratios is about -13% (Figure 7).

21   The smaller model bias for ^{7}Be/^{210}Pb ratios than for ^{7}Be concentrations reflects the fact that the

22   ratio cancels out the errors in precipitation scavenging (Koch et al. 1996) that contribute to the

23   underestimate of ^{210}Pb and ^{7}Be activities. On the other hand, the negative model bias for the

24   ^{7}Be/^{210}Pb ratio again points to weak downward mixing from the free troposphere.

Atmospheric
Chemistry
and Physics
Discussions

1   If one compares the month-to-month variation of ^{210}Pb and ^{7}Be (Figures 5 and 6) and

2   precipitation in the model (Figure 4), the maxima/minima of precipitation appear to be in phase

3   with those of both radionuclides' activities. This reflects the effects of precipitation scavenging

4   on radionuclide aerosols.

5   We conducted model sensitivity experiments where convection (transport and

6   scavenging), wet scavenging due to both large-scale and convective precipitation, and dry

7   deposition processes are turned off, respectively, to examine the roles of these processes in

8   controlling the seasonality of ^{210}Pb and ^{7}Be at Mt. Cimone. Figure 8 shows the results for the

9   standard and sensitivity runs at the "grid to the south of "ij", for which the simulated tracer

10   seasonal variations are similar to those observed, while the monthly percentage deviations from

11   the annual mean concentrations are shown in SI Figure 3. Figures 9-12 show maps of simulated

12   changes in ^{210}Pb and ^{7}Be concentrations when convection or wet scavenging is turned off.

13   Turning off dry deposition does not significantly change the simulated ^{210}Pb and ^{7}Be

14   concentrations, partly due to sampling the higher vertical gridbox in the model (larger effects

15   are seen at the bottom model layer). Turning off convection (i.e., with neither convective

16   transport nor convective scavenging), the simulated ^{7}Be seasonality also remains nearly the

17   same. This suggests the compensating effects between subsidence (increasing ^{7}Be) associated

18   with convective transport and scavenging (decreasing ^{7}Be) due to convective precipitation. In

19   the case of ^{210}Pb, turning off convection does not change the seasonal pattern but generally

20   results in larger ^{210}Pb concentrations and particularly during summer/autumn when convective

21   transport is more important at the site. In fact, no convective transport of ^{222}Rn (SI Figure 5)

22   results in less ^{222}Rn (and ^{210}Pb) being transported to the free troposphere, but also more ^{210}Pb

23   available in PBL lifted to the free troposphere by large-scale vertical transport; on the other

24   hand, lack of convective scavenging of ^{210}Pb increases its concentration in the free troposphere.

25   Turning off convection therefore results in an increase of ^{210}Pb concentrations in the free

Atmospheric
Chemistry
and Physics
Discussions

1   troposphere. Both surface ^{222}Rn concentrations at the elevation of Mt. Cimone (SI Figure 4),

2   as well as a map of changes in ^{210}Pb concentrations due to convection in the model (Figure 9)

3   show that convection in the region is more important during summer and autumn, but is not

4   negligible during spring, possibly due to thermal inertia.

5   The model run without scavenging suggests that, apart from downward transport from

6   the upper troposphere and lower stratosphere, wet scavenging is mainly responsible for the

7   seasonal variation of ^{7}Be (Figure 8, bottom panel). None of our simulations is able to describe

8   the observed ^{7}Be summertime peak, suggesting that the local circulation in this region with

9   complex topography may not be resolved by the coarse-resolution model. For ^{210}Pb (Figure 8,

10   top panel), it appears that wet scavenging plays a more important role during August-December

11   than during January-July. This appears to be associated with the seasonality of precipitation,

12   which shows prolonged elevated values during August-December, as well as a maximum

13   during April, as previously discussed (Figure 5). A plot of changes in ^{210}Pb concentrations due

14   to scavenging in the model (Figure 10) confirms that the scavenging effect is larger during fall

15   and, to a lesser extent, during summer. At Mt. Cimone, the scavenging effect is not minimal

16   during July (month of minimum precipitation, Figure 4), suggesting the influence of

17   precipitation scavenging elsewhere in the region on the site.

18   **6 Summary and Conclusions**

19   We have used a global 3-D model (GMI CTM) driven by the MERRA assimilated

20   meteorological data from NASA's GMAO to simulate the ^{210}Pb and ^{7}Be observations from the

21   Mt. Cimone (44°12' N, 10°42' E, 2165 m asl, Italy) WMO-GAW station in 2005. The two

22   natural atmospheric radionuclides originate from contrasting source regions (lower troposphere

23   and upper troposphere/lower stratosphere, respectively), attach to submicron particles, and are

24   removed from the troposphere mainly by wet deposition. Our objective was to examine the

25   roles of horizontal advection, vertical transport (large-scale and convection), and wet

Atmospheric
Chemistry
and Physics
Discussions

1   scavenging in determining the seasonality of ^{210}Pb and ^{7}Be at Mt. Cimone. The observed ^{210}Pb

2   concentrations are characterized by maxima in summer and minima during the cold period.

3   The seasonality of ^{7}Be is more complex, with a major peak in summer, a secondary peak in

4   spring and a minimum in winter. This is the first modeling study of ^{210}Pb and ^{7}Be observations

5   at Mt. Cimone. This site is representative of free-tropospheric Southern Europe/Mediterranean

6   conditions most of the year, and as such the comparison between measurements and

7   simulations can serve as an indication of shortcomings in the model or in the meteorological

8   data.

9   Precipitation and wind fields are important to the model's performance in representing

10   the transport and scavenging processes. We evaluated the MERRA precipitation field used by

11   GMI CTM against the GPCP satellite and surface observations, and a generally good

12   agreement was found. The seasonality of precipitation at Mt. Cimone shows increased amounts

13   during April and the period of August-December, and minimum in June-July. The MERRA

14   assimilated winds at the low resolution version we used captured the main circulation patterns

15   (e.g., location of the Azores high pressure, location of the ITCZ) in the Northern Hemisphere.

16   However, some local-scale winds and pressure systems, which are important for transport to

17   the sampling site, were likely not well resolved at the coarse resolution we used. A general

18   good agreement was found between the MERRA assimilated wind fields and the main

19   advection patterns at the site (e.g., prevalence of long-range transport from Western Europe,

20   North America and Arctic region during the cold season, as opposed to the prevailing regional

21   transport during the warm season).

22   The model well reproduced the observed ^{210}Pb seasonality: ^{210}Pb maxima during the

23   warm period were attributed to the stronger (thermal) convection, which uplifts more ^{222}Rn

24   (and ^{210}Pb) from the boundary layer. The model is less successful in reproducing the observed

25   ^{7}Be seasonality. ^{7}Be was better represented during the cold period, while the observed summer

Atmospheric
Chemistry
and Physics
Discussions

1 ^{7}Be maximum was underestimated by the model. The model underestimate of ^{7}Be levels in the

2 warm months is partly due to the sensitivity to spatial sampling in the model, but also suggests

3 that the mixing of air masses between the PBL and the lower free troposphere is likely too

4 weak. This suggests that additional work comparing the model results with more surface

5 observations is needed in order to better understand this effect. The simulated lower annual

6 average ^{7}Be concentration relative to the observation is also partly attributed to the fact that the

7 model used the ^{7}Be production rate for a solar maximum year, while in 2005 (our simulation

8 year) the solar activity was rather low.

9 By examining the wind fields and horizontal distribution of radiotracers in the model, we

10 noted that the sampling site is in a location where there is a large gradient, especially in the

11 North-South direction. Accordingly, we investigated the sensitivity of model results to spatial

12 sampling. A better agreement between the model and the observations at some adjacent

13 gridboxes was found. The ^{7}Be March maximum was linked to the large stratospheric influence

14 during winter/spring. The model tends to underestimate the summertime ^{210}Pb and ^{7}Be, but

15 better simulates the ^{7}Be/^{210}Pb ratio because the model errors due to precipitation scavenging

16 appear to be canceled out in the ratio.

17 We have conducted a series of model sensitivity experiments to further examine and

18 quantify the roles of wet scavenging, dry deposition, and convection (transport and scavenging)

19 in controlling the seasonality of ^{210}Pb and ^{7}Be at Mt. Cimone. Dry deposition does not have a

20 significant effect on the magnitude and seasonality of ^{210}Pb and ^{7}Be concentrations at the site.

21 The relatively weak combined effects of convective transport and convective scavenging on

22 the radiotracer seasonality were attributed to the compensating effects of convective transport

23 and convective scavenging on tracer concentrations in the lower free troposphere (at the

24 elevation of Mt. Cimone). Convection appears to be more important to the regional distribution

25 of both radiotracers during summer and autumn, although it is also significant during spring.

Atmospheric
Chemistry
and Physics
Discussions

1   Finally, scavenging is found to be the most important process controlling the seasonal

2   variations of ^{210}Pb and ^{7}Be at Mt. Cimone. For ^{210}Pb, precipitation plays a more important role

3   during August-December than during January-July. This was attributed to the seasonality of

4   local and regional precipitation, which shows prolonged elevated values in the period of

5   August-December.

6   While our simulations demonstrated some capabilities of the model to reproduce the

7   seasonality of ^{210}Pb and ^{7}Be, they highlight the weaknesses of the model in reproducing local

8   features, presumably due to its coarse resolution. Model simulations at a higher resolution

9   would improve this model analysis of ^{210}Pb and ^{7}Be observations at Mt. Cimone, a high-

10   elevation site. The understanding of downward transport associated with convection during

11   summer also requires improving. As such, ^{210}Pb and ^{7}Be tracers will prove to be very useful in

12   our understanding of seasonal behaviors of other environmentally important trace gases and

13   aerosols at Mt. Cimone. Since other aerosols and trace gases (e.g., black carbon, CO, O_3) are

14   also measured at the station, we plan to conduct comparisons between model simulations and

15   those measurements to corroborate or contrast with the radionuclide results.

16

Data availability

18   A description of the observational data and model output used in this paper can be found in

19   Sect. 2 and they are available upon request by contacting Laura Tositti (laura.tositti@unibo.it)

20   and Hongyu Liu (hongyu.liu-1@nasa.gov), respectively.

21

Atmospheric
Chemistry
and Physics
Discussions

13

References

15   Arimoto, R., Snow, J.A., Graustein, W.C., Moody, J.L., Ray, B.J., Duce, R.A., Turekian, K.K.,

16   and Maring H.B.: Influences of atmospheric transport pathways on radionuclide activities

17   in aerosol particles from over the North Atlantic, J Geophys Res, 104(D17), 301-321, 1999.

18   Balkanski, Y, Jacob, D.J., Gardner, G.M., Graustein, W., Turekian, K.K.: Transport and

19   residence times of tropospheric aerosols inferred from a global three-dimensional

20   simulation of ^{210}Pb, J Geophys Res, 98 (D11), 20573-20586, 1993.

21   Baskaran, M.: Po-210 and Pb-210 as atmospheric tracers and global atmospheric Pb-210

22   fallout: a review, J Environ Radioactiv, 102, 500-513, 2011.

23   Beer, J., McCracken, K., and von Steiger, R.: Cosmogenic radionuclides. Springer, Heidelberg,

24   Germany, 2012.

Bonasoni, P., Evangelisti, F., Bonafé, U., Feldmann, H., Memmesheimer, M., Stohl, A., and Tositti, L.: Stratosphere-troposphere exchanges: case studies recorded at Mt. Cimone during VOTALP project, Phys Chem Earth (C), 24(5), 443-446, 1999.

Bonasoni, P., Evangelisti, F., Bonafé, U., Ravegnani, F., Calzolari, F., Stohl, A., Tositti, L,. Tubertini, O., and Colombo, T.: Stratospheric ozone intrusion episodes recorded at Mt. Cimone during VOTALP project: Case studies, Atmos Environ, 34, 1355-1365, 2000a.

Bonasoni, P., Stohl, A., Cristofanelli, P., Calzolari, F., Colombo, T., and Evangelisti, F.: Background ozone variations at Mt Cimone station, Atmos Environ, 34, 5183-5189, 2000b.

Bourcier, L., Masson, O., Laj, P., Pichon, J.M., Paulat, P., Freney, E., and Sellegri, K.: Comparative trends and seasonal variation of ^{7}Be, ^{210}Pb and ^{137}Cs at two altitude sites in the central part of France, J Environ Radioactiv, 102, 294-301, 2011.

Brattich, E., Hernandéz-Ceballos, M.A., Cinelli, G., and Tositti, L.: Analysis of peak ^{210}Pb values at Mt. Cimone (1998-2011), Atmos Environ, 112, 136-147, 2015.

Brattich, E., Orza, J.A.G., and Tositti, L.: Advection patterns at the WMO-GAW station of Mt. Cimone: seasonality, trends, and influence on atmospheric composition, manuscript in preparation, 2016.

Brost, R.A., Feichter, J., and Heimann, H.: Three-dimensional simulation of ^{7}Be in a global climate model, J Geophys Res, 96, 22423-22445, 1991.

Burlando, M.: The synoptic-scale surface wind climate regimes of the Mediterranean Sea according to the cluster analysis of ERA-40 wind fields, Theor Appl Climatol, 96, 69-83, 2009.

Burlando, M., Antonelli, M., and Ratto, C.F.: Mesoscale wind climate analysis: identification of anemological regions and wind regimes, Int J Climatol, 28, 629-641, 2008.

Atmospheric
Chemistry
and Physics
Discussions

Open Access

1   Caillet, S., Arpagaus, P., Monna, F., and Dominik, J.: Factors controlling [7]Be and [210]Pb

2   atmospheric deposition as revealed by sampling individual rain events in the region of

3   Geneva, Switzerland, J Environ Radioactiv, 53, 241-256, 2001.

4   Campins, J., Jansà, A., and Genovés, A.: Three-dimensional structure of western

5   Mediterranean cyclones, Int J Climatol, 26, 323-343, 2006.

6   Cannizzaro, F., Greco, G., Raneli, M., Spitale, M.C., and Tomarchio, E.: Concentration

7   measurements of [7]Be at ground level air at Palermo, Italy – comparison with solar activity

8   over a period of 21 years, J Environ Radioactiv, 84, 457-467, 2004.

9   Carvalho, A.C., Reis, M., Silva, L., and Madruga, M.J.: A decade of [7]Be and ^{210}Pb activity in

10   surface aerosols measured over the Western Iberian Peninsula, Atmos Environ, 67, 193-

11   202, 2013.

12   Ciattaglia, L.: Interpretation of atmospheric CO_2 measurements at Mt. Cimone (Italy) related

13   to wind data. Journal of Geophysical Research 88, C2, 1331-1338, 1983.

14   Ciattaglia, L., Cundari, V., and Colombo, T.: Further measurements of atmospheric carbon

15   dioxide at Mt. Cimone, Italy: 1979-1985, Tellus B, 39, 13-20, 1987.

16   Colombo, T., Santaguida, R., Capasso, A., Calzolari, F., Evangelisti, F., and Bonasoni, P.:

17   Biospheric influence on carbon dioxide measurements in Italy, Atmos Environ, 34, 4963-

18   4969, 2000.

19   Considine, D.B., Douglass, A.R., Connell, P.S., Kinnison, D.E., and Rotman, D.A.: A polar

20   stratospheric cloud parameterization for the global modeling initiative three-dimensional

21   model and its response to stratospheric aircraft, J Geophys Res, 105(D3), 3955-3973, 2000.

22   Considine, D.B., Connell, P.S., Logan, J.A.: Simulating ozone in the near tropopause region

23   with a new combined model of the stratosphere and troposphere, in: Quadrennial Ozone

24   Symposium QOS 2004, edited by: Zerefos, C, International Ozone Commission, Kos,

25   Greece, pp. 739-740, 2004.

Atmospheric
Chemistry
and Physics
Discussions

1 Considine, D.B., Bergmann, D.J., and Liu, H.: Sensitivity of Global Modeling Initiative

2   chemistry and transport model simulations of radon-222 and lead-210 to input

3   meteorological data, Atmos Chem Phys, 5, 3389-3406, 2005.

4 Cristofanelli, P., Bonasoni, P., Collins, W., Feichter, J., Forster, C., James, P., Kentarchos, A.,

5   Kubik, P.W., Land, C., Meloen, J., Roelofs, G.J., Siegmund, P., Sprenger, M., Schnabel,

6   C., Stohl, A., Tobler, L., Tositti, L., Trickl, T., and Zanis, P.: Stratosphere-to-troposphere

7   transport: A model and method evaluation, J Geophys Res, 108(D12), 8525,

8   doi:10.1029/2002JD002600, 2003.

9 Cristofanelli, P., Bonasoni, P., Tositti, L., Bonafé, U., Calzolari, F., Evangelisti, F., Sandrini,

10   S., and Stohl, A.: A 6-year analysis of stratospheric intrusions and their influence on ozone

11   at Mt. Cimone (2165 m above sea level), J Geophys Res, 111, D03306,

12   doi:10.1029/2005JD006553, 2006.

13 Cristofanelli, P., Bonasoni, P., Carboni, G., Calzolari, F., Casarola, L., Zauli Sajani, S., and

14   Santaguida, R.: Anomalous high ozone concentrations recorded at a high mountain station

15   in Italy in summer 2003, Atmos Environ, 41, 1383-1394, 2007.

16 Cristofanelli, P., Calzolari, F., Bonafé, U., Duchi, R., Marinoni, A., Roccato, F., Tositti, L., and

17   Bonasoni P.: Stratospheric intrusion index (SI^2) from baseline measurement data, Theor

18   Appl Climatol, 97, 317-325, 2009a.

19 Cristofanelli, P., Marinoni, A., Arduini, J., Bonafé, U., Calzolari, F., Colombo, T., Decesari,

20   S., Duchi, R., Facchini, M.C., Fierli, F., Finessi, E., Maione, M., Chiari, M., Calzolai, G.,

21   Messina, P., Orlandi, E., Roccato, F., and Bonasoni, P.: Significant variations of trace gas

22   composition and aerosol properties at Mt. Cimone during air mass transport from North

23   Africa – contributions from wildfire emissions and mineral dust, Atmos Chem Phys, 9,

24   4603-4619, 2009b.

Atmospheric
Chemistry
and Physics
Discussions

1   Cristofanelli, P., Scheel, H.-E., Steinbacher, M., Saliba, M., Azzopardi, F., Ellul, R., Fröhlich,

2   M., Tositti, L., Brattich, E., Maione, M., Calzolari, F., Duchi, R., Landi, T.C., Marinoni,

3   A., and Bonasoni, P.: Long-term surface ozone variability at Mt. Cimone WMO/GAW

4   global station (2165 m a.s.l., Italy), Atmos Environ, 101, 23-33, 2015.

5   Cuevas, E., Gonzalez, Y., Rodríguez, S., Guerra, J.C., Gómez-Peláez, A.J., Alonso-Pérez, S.,

6   Bustos, J., and Milford, C.: Assessment of atmospheric processes driving ozone variations

7   in the subtropical North Atlantic free troposphere, Atmos Chem Phys, 13, 1973-1998, 2013.

8   Daish, S.R., Dale, A.A., Dale, C.J., May, R., and Rowe, J.E.: The temporal variations of [7]Be,

9   [210]Pb and [210]Po in England, J Environ Radioactiv, 84, 457-467, 2005.

10   Dibb, J.E., Talbot, R.W., and Gregory, G.L.: Beryllium 7 and lead 210 in the western

11   hemisphere Arctic atmosphere: Observations from three recent aircraft-based sampling

12   programs, J Geophys Res, 97, 16709-16715, 1992.

13   Dibb, J.E., Meeker, L.D., Finkel, R.C., Southon, J.R., Caffee, M.W., and Barrie, L.A.:

14   Estimation of stratospheric input to the Arctic troposphere: [7]Be and [10]Be in aerosols at

15   Alert, Canada, J Geophys Res, 99, 12855-12864, 1994.

16   Dibb, J.E.: Vertical mixing above Summit, Greenland: insights into seasonal and high

17   frequency variability from the radionuclide tracers [7]Be and ^{210}Pb, Atmos Environ, 41, 5020-

18   5030, 2007.

19   Dueñas, C., Fernández, M.C., Cañete, S., and Pérez, M.: [7]Be to ^{210}Pb concentration ratio in

20   ground level air in Málaga (36.7°N, 4.5°W), Atmos Res, 92, 49-57, 2009.

21   Dueñas, C., Orza, J.A.G., Cabello, M., Fernández, M.C., Cañete, S., Pérez, M., and Gordo, E.:

22   Air mass origin and its influence on radionuclide activities ([7]Be and ^{210}Pb) in aerosol

23   particles at a coastal site in the western Mediterranean, Atmos Res, 101, 205-214, 2011.

24   Duncan, B.N., Strahan, S.E., and Yoshida, Y.: Model study of the cross-tropopause transport

25   of biomass burning pollution, Atmos Chem Phys, 7, 3713-3736, 2007.

Atmospheric
Chemistry
and Physics
Discussions

Open Access

EGU

1   Duncan, B.N., West, J.J., Yoshida, Y., Fiore, A.M., and Ziemke, J.R.: The influence of

2   European pollution on ozone in the Near East and northern Africa, Atmos Chem Phys, 8,

3   2267-2283, doi:10.5194/acp-8-2267-2008, 2008.

4   Feely, H.W., Larsen, R.J., and Sanderson, C.G.: Factors that cause seasonal variations in

5   beryllium-7 concentrations in surface air, J Environ Radioactiv, 9, 223-249, 1989.

6   Fischer, H., Kormann, R., Klüpfel, T., Gurk, C., Königstedt, R., Parchatka, U., Mühle, J., Rhee,

7   T.S., Brenninkmeijer, C.A.M., Bonasoni, P., and Stohl, A.: Ozone production and trace gas

8   correlations during the June 2000 MINATROC intensive measurement campaign at Mt.

9   Cimone. Atmos Chem Phys, 3, 725-738, 2003.

10 Forster, P., Ramaswamy, V., Artaxo, P., Berntsen, T., Betts, R., Fahey, D.W., Haywood, J.,

11   Lean, J., Lowe, D.C., Myhre, G., Nganga, J., Prinn, R., Raga, G., Schulz, M., and Van

12   Dorland, R.: Changes in Atmospheric Constituents and in Radiative Forcing, in Climate

13   Change 2007: The Physical Science Basis. Contribution of Working Group I to the Fourth

14   Assessment Report of the Intergovernmental Panel on Climate Change, [Solomon, S., Qin,

15   D., Manning, M., Chen, Z., Marquis, M., Averyt, K.B., Tignor, M., and Miller, H.L. (eds.)],

16   Cambridge University Press, Cambridge, United Kingdom and New York, NY, USA, 2007.

17 Froehlich, K., and Masarik, J.: Radionuclides as tracers and timers of processes in the

18   continental environment – Basic concepts and methodologies. In: Radioactivity in the

19   Environment, 16, Chapter 2, 27-50, Environmental Radionuclides: Tracers and Timers of

20   Terrestrial Processes. Edited by Elsevier. doi:10.1016/S1569-4860(09)01602-7, 2010

21 Gaffney, J.S, Marley, N., and Cunningham, M.M.: Natural radionuclides in fine aerosols in the

22   Pittsburgh area, Atmos Environ, 38, 3191-3200, 2004.

23 Gäggeler, H.W.: Radioactivity in the atmosphere, Radiochim Acta, 70-71, 345-353, 1995.

24 Gerasopoulos, E., Zanis, P., Stohl, A., Zerefos, C.S., Papastefanou, C., Ringer, W., Tobler, L.,

25   Hübener, S., Gäggeler, H.W., Kanter, H.J., Tositti L., and Sandrini, S.:A climatology of

Atmospheric
Chemistry
and Physics
Discussions

1   [7]Be at four high-altitude stations at the Alps and the Northern Apennines, Atmos Environ,

2   35, 6347-6360, 2001.

3   Gerasopoulos, E.,Zanis, P., Zerefos, C.S., Papastefanou, C., Ringer, W., Gäggeler, H.W.,

4   Tobler, L., and Kanter, H.J.,: Factors and processes controlling the concentration of the

5   cosmogenic radionuclide [7]Be at high-altitude Alpine stations, In: Radioactivity in the

6   Environment, Volume 7, 863-870, Elsevier Ltd., ISSN 1569-4860, DOI10.1016/S1569-

7   4860(04)07108-6, 2005.

8   Graustein, W.C., and Turekian, K.K.: Radon fluxes from soils to the atmosphere

9   measured by ^{210}Pb-^{226}Ra disequilibrium in soils, Geophys Res Lett, 17, 841-844,

10   1990.

11   Graustein, W.C., and Turekian, K.K.: [7]Be and ^{210}Pb indicate an upper troposphere source for

12   elevated ozone in the summertime subtropical free troposphere of the eastern North

13   Atlantic, Geophys Res Lett, 23, 539-542, 1996.

14   Hötzl, H., and Winkler, R.: Activity concentrations of ^{226}Ra, ^{228}Ra, ^{210}Pb, ^{40}K and [7]Be and their

15   temporal variations in surface air, J Environ Radioactiv, 5, 445-458, 1987

16   Huang M., Carmichael, G.R., Chai, T., Pierce, R.B., Oltmans, S.J., Jaffe, D.A., Bowman, K.W.,

17   Kaduwela, A., Cai, C., Spak, S.N., Weinheimer, A.J., Huey, L.G., and Diskin, G.S.:

18   Impacts of transported background pollutants on summertime western US air quality:

19   model evaluation, sensitivity analysis and data assimilation, Atmos Chem Phys, 13, 359-

20   391, 2013.

21   Ioannidou, A., Manolopoulou, M., and Papastefanou, C.: Temporal changes of [7]Be and ^{210}Pb

22   concentrations in surface air at temperate latitudes (40°), Appl Radiat Isotopes, 63(2), 277-

23   284, 2005.

24   Ioannidou, A., Vasileiadis, A., and Melas, D.: Time lag between the tropopause height and [7]Be

25   activity concentrations in surface air, J Environ Radioactiv, 129, 80-85, 2014.

Atmospheric
Chemistry
and Physics
Discussions

Jacob, D.J., and Prather, M.J.: Radon-222 as a test of boundary layer convection in a general circulation model, Tellus B, 42, 118-134, 1990.

James, P., Stohl, A., Forster, C., Eckhardt, S., Seibert, P., and Frank, A., A 15-year climatology of stratosphere-troposphere exchange with a Lagrangian particle dispersion model 2. Mean climate and seasonal variability, J Geophys Res, 108(D12), 8522, doi:10.1029/2002JD002639, 2003.

Jasiulionis, R., and Wershofen, H.: A study of the vertical diffusion of the cosmogenic radionuclides, ^{7}Be and ^{22}Na in the atmosphere. J Environ Radioactiv, 79, 157-169, 2005.

Johnson, W., and Viezee, W., Stratospheric ozone in the lower troposphere: i. Presentation and interpretation of aircraft measurements. Atmos Environ, 15, 1309–1323, 1981.

Junge, C.E.: Air chemistry and radioactivity. Academic Press, New York, USA, and London, UK, 382 pp, 1963.

Kinnison, D.E., Connell, P.S., Rodriguez, J.M., Rotman, D.A., Considine, D.B., Tannahill, J., Ramaroson, R., Rasch, P.J., Douglass, A.R., Baughcum, S.L., Coy, L., Waugh, D.W., Kawa, S.R., and Prather, M.J.: The Global Modeling Initiative assessment model: Application to high-speed civil transport perturbation, J Geophys Res, 106(D2), 1693-1711, 2001.

Koch, D.M., Jacob, D.J., and Graustein, W.C.: Vertical transport of tropospheric aerosols as indicated by ^{7}Be and ^{210}Pb in a chemical tracer model, J Geophys Res, 101(D13), 18651-18666, 1996.

Koch, D., and Rind, D.: Beryllium10/beryllium7 as a tracer of stratospheric transport, J Geophys Res, 103, 3907-3917, 1998.

Kulan, A., Aldahan, A., Possnert, G., and Vintersved, I.: Distribution of ^{7}Be in surface air of Europe, Atmos Environ, 40, 3855-3868, 2006.

Atmospheric
Chemistry
and Physics
Discussions

1   Lal, D., Malhotra, P.K., and Peters, B.: On the production of radioisotopes in the atmosphere

2   by cosmic radiation and their application to meteorology, J Atmos Sol-Terr Phy, 12, 306-

3   328, 2006.

4   Lal, D., and Peters, B.: Cosmic ray produced radioactivity on the Earth, in: Handbuch der

5   Physik, 46/2, edited by Sitte, K., Springer-Verlag, New York, USA, pp. 551-561, 1967.

6   Lee, H.N., Wan, G., Zheng, X., Sanderson, C.G., Josse, B., Wang, S., Yang, W., Tang, J.,and

7   Wang, C.: Measurements of ^{210}Pb and ^{7}Be in China and their analysis accompanied with

8   global   model   calculations   of ^{210}Pb,   J   Geophys   Res,   109,   D22203,

9   doi:10.1029/2004JD005061, 2004.

10 Lee, H.N., Tositti, L., Zheng, X., and Bonasoni, P.: Analyses and comparisons of variations of

11   ^{7}Be, ^{210}Pb and ^{7}Be/^{210}Pb with ozone observations at two Global Atmosphere Watch stations

12   from high mountains, J Geophys Res, 112, D05303, doi:10.1029/2006JD007421, 2007

13 Lelieveld, J., Berresheim, H., Borrman, S., Crutzen, P.J., Dentener, F.J., Fischer, H., Feichter,

14   J., Flatau, P.J., Heland, J., Holzinger, R., Korrmann, R., Lawrence, M.G., Levin, Z.,

15   Markowicz, K.M., Mihapoulos, N., Minikin, A., Ramanathan, V., de Reus, M., Roelofs,

16   G.J., Scheeren, H.A., Sciare, J., Schlager, H., Schultz, M., Siegmund, P., Steil, B.,

17   Stephanou, E.G., Stier, P., Traub, M., Warneke, C., Williams, J., and Ziereis, H.: Global

18   air pollution crossroads over the Mediterranean. Science, 298, 794-799, 2002.

19 Li, Q., Jacob, D.J., Logan, J.A., Bey, I., Yantosca, R.M., Liu, H., Martin, R.V., Fiore, A.M.,

20   Field, B.D., Duncan, B.N.: A Tropospheric Ozone Maximum Over the Middle East,

21   Geophys Res Lett, 28(17), 3235-3238, 2001.

22 Likuku, A.S.: Factors influencing ambient concentrations of ^{210}Pb and ^{7}Be over the city of

23   Edinburgh (55.9°N, 03.2°W), J Environ Radioactiv, 87, 289-304, 2006.

Atmospheric
Chemistry
and Physics
Discussions

1   Liu, H., Jacob, D.J., Bey, I., and Yantosca, R.M.: Constraints from the ^{210}Pb and ^{7}Be on wet

2   deposition and transport in a global three-dimensional chemical tracer model driven by

3   assimilated meteorological fields, J Geophys Res, 106, D11, 12109-12128, 2001.

4   Liu, H., Jacob, D.J., Dibb, J.E., Fiore, A.M., and Yantosca, R.M.: Constraints on the sources

5   of tropospheric ozone from ^{210}Pb-^{7}Be-O$_3$ correlations, J Geophys Res, 109(D07306),

6   doi:10.1029/2003JD003988, 2004.

7   Liu, H., Considine, D. B., Horowitz, L. W., Crawford, J. H., Rodriguez, J. M., Strahan, S. E.,

8   Damon, M. R., Steenrod, S. D., Xu, X., Kouatchou, J., Carouge, C., and Yantosca, R. M.:

9   Using beryllium-7 to assess cross-tropopause transport in global models, Atmos. Chem.

10   Phys., 16, 4641-4659, doi:10.5194/acp-16-4641-2016, 2016.

11 Lozano, R.L., Hernandéz-Ceballos, M.A., San Miguel, E.G., Adame, J.A., and Bolívar, J.P.:

12   Meteorological factors influencing the ^{7}Be and ^{210}Pb concentrations in surface air from the

13   southwestern Iberian Peninsula, Atmos Environ, 63, 168-178, 2012.

14 Lozano, R.L., Hernandéz-Ceballos, M.A., Rodrigo, J.F., San Miguel, E.G., Casas-Ruiz, M.,

15   García-Tenorio, R., and Bolívar, J.P.: Mesoscale behavior of ^{7}Be and ^{210}Pb in superficial

16   air along the Gulf of Cadiz (south of Iberian peninsula), Atmos Environ, 80, 75-84, 2013.

17 Marinoni, A., Cristofanelli, P., Calzolari, F., Roccato, F., Bonafé, U., and Bonasoni, P.:

18   Continuous measurements of aerosol physical parameters at the Mt. Cimone GAW Station

19   (2165 m asl, Italy), Sci Total Environ, 391, 241-251, 2008.

20 Millàn, M., Sanz, J., Salvador, R., and Mantilla, E.: Atmospheric dynamics and ozone cycles

21   related to nitrogen deposition in the western Mediterranean, Environ Pollut, 118, 167-186,

22   2006.

23 Monks, P.S., Granier, C., Fuzzi, S., Stohl, A., Williams, M.L., Akimoto, H., Amann, M.,

24   Baklanov., A., Baltensperger, U., Bey, I., Blake, N., Blake, R.S., Carslaw, K., Cooper,

25   O.R., Dentener, F., Fowler, D., Fragkou, E., Frost, G.J., Generoso, S., Ginoux, P., Grewe,

V., Guenther, A., Hansson, H.C., Henne, S., Hjorth, J., Hofzumahaus, A., Huntrieser, H., Isaksen, I.S.A., Jenkin, M.E., Kaiser, J., Kanakidou, M., Klimont, Z., Kulmala, M., Laj, P., Lawrence, M.G., Lee, J.D., and Liousse, C.: Atmospheric composition change – global and regional air quality, Atmos Environ, 43, 5268-5350, 2009.

Moore, H.E., Poet, S.E., and Martell, E.A.: ^{222}Rn, ^{210}Pb, ^{210}Bi, and ^{210}Po, profiles and aerosol residence times versus altitude, J Geophys Res, 78, 7065-7075, 1973.

Nazaroff, W.W.: Radon transport from soil to air, Rev Geophys, 30, 137-160, 1992.

ORTEC: Gamma-Vision 32 A66-B32 user's manual. ORTEC USA, Part No. 783620, Manual Revision D, 2003.

Papastefanou, C., and Ioannidou, A.: Aerodynamic size association of ^{7}Be in ambient aerosols. J Environ Radioactiv, 26, 273-282, 1995.

Pham, M.K., Betti, M., Nies ,H., and Povinec, P.P.: Temporal changes of ^{7}Be, ^{137}Cs and ^{210}Pb activity concentrations in surface air at Monaco and their correlation with meteorological parameters, J Environ Radioactiv, 102, 1045-1054, 2011.

Rastogi, N., and Sarin, M.M.: Atmospheric ^{210}Pb and ^{7}Be in ambient aerosols over low- and high-altitude sites in 34 semiarid region: Temporal variability and transport processes, J Geophys Res, 113, doi:10.1029/2007JD009298, 2008.

Rehfeld, S., and Heimann, M.: Three dimensional atmospheric transport simulation of the radioactive tracers ^{210}Pb, ^{7}Be, ^{10}Be, and ^{90}Sr, J Geophys Res, 100 (D12), 26141-26161, 1995.

Reiter, E.R.: Weather phenomena of the Mediterranean basin. Part 1. General description of the meteorological processes, In: Handbook for forecasters in the Mediterranean basin, Environment Prediction Research Facility, Naval Postgraduate School, Monterey, California, U.S. Department of Commerce, available at http://www.dtic.mil/cgi-bin/GetTRDoc?AD=ADA024271, last accessed 15 March 2016, 1975.

Atmospheric
Chemistry
and Physics
Discussions

1   Reiter, R., Sladkovich, K., Pötzl, K., Carnuth, W., and Kanter H.J.: Studies on the influx of

2   stratospheric air into the lower troposphere using cosmic-ray produced radionuclides and

3   fallout, Arch Meteor Geophy A, Vol.20(3), 211-246, 1971.

4   Reiter, R., Munzert, K., Kanter, H.-J., and Pötzl, K.: Cosmogenic radionuclides and ozone at a

5   mountain station at 3.0 km a.s.l., Arch Meteor Geophy B, 32, 131-160, 1983.

6   Rienecker, M.M., Suarez, M.J., Gelaro, R., Todling, R., Bacmeister, J., Liu, E., Bosilovich,

7   M.G., Schubert, S.D., Takacs, L., Kim, G.-K., Bloom, S., Chen, J., Collins, D., Conaty, A.,

8   da Silva, A., Gu, W., Joiner, J., Koster, R.D., Lucchesi, R., Molod, A., Owens, T., Pawson,

9   S., Pegion, P., Redder, C.R., Reichle, R., Robertson, F.R., Ruddick, A.G., Sienkewicz, M.,

10   and Woollen, J.: MERRA: NASA's Modern-Era Retrospective Analysis for Research and

11   Applications. J Climate, 24(14), 3624-3648, 2011.

12 Rodriguez, J.M., Logan, J.A., Bergmann, D., Megretskaia, I., Jacob, D.J., Xie, H., Das, B., and

13   Strahan, S.E.: The impact of meteorological fields on tropospheric ozone distributions

14   calculated by the Global Modeling Initiative (GMI) chemical-transport model, in:

15   Quadrennial Ozone Symposium QOS 2004, edited by: Zerefos, C., pp.147, International

16   Ozone Commission, Kos, Greece, 2004

17 Rotman, D.A., Tannahill, J.R., Kinnison, D.E., Connell, P.S., Bergmann, D., Proctor, D.,

18   Rodriguez, J.M., Lin, S.J., Rood, R.B., Prather, M.J., Rasch, P.J., Considine, D.B.,

19   Ramaroson, R., and Kawa, S.R.: Global Modeling Initiative assessment model: Model

20   description, integration, and testing of the transport shell, J Geophys Res, 106(D2), 1669-

21   1691, 2001.

22 Schery, S.D., Whittlestone, S., Hart, K.P., and Hill, S.E.: The flux of radon and thoron from

23   Australian soils, J Geophys Res, 100, 26141-26161, 1989.

24 SILSO (Sunspot Index and Long-term Solar Observation), World Data Center – Sunspot

25   Number and Long-Term Solar Observations, Royal Observatory of Belgium, on-line

Atmospheric
Chemistry
and Physics
Discussions

1   Sunspot Number catalogue, available at http://sidc.oma.be/silso/, last accessed 15 March

2   2016

3   Simon, J., Meresova, J., Sykora, I., Jeskovsky, M., and Holy, K.: Modeling of temporal

4   variations of vertical concentration profile of ^{7}Be in the atmosphere. Atmos Environ, 43,

5   2000-2004, 2009.

6   Steinmann, P., Zeller, M., Beuret, P., Ferreri, G., and Estier, S.: Cosmogenic ^{7}Be and ^{22}Na in

7   ground level air in Switzerland (1994-2011), J Environ Radioactiv, 124, 68-73, 2013.

8   Stohl, A., Wernli, H., James, P., Borqui, M., Forster, C., Liniger, M.A., Seibert, P., and

9   Sprenger, M.: A new perspective of stratosphere-troposphere exchange, Bull Am Meteor

10   Soc, 84, 1565-1573 DOI: 10.1175/BAMS-84-11-1565, 2003.

11   Strahan, S.E., Duncan, B.N., and Hoor, P.: Observationally-derived diagnostics of transport in

12   the lowermost stratosphere and their application to the GMI chemistry transport model.

13   Atmos Chem Phys, 7, 1435-2445, 2007

14   Todorovic, D., Popovic, D., Djuric, G., Radenkovic, M.: ^{7}Be to ^{210}Pb concentration ratio in

15   ground level air in Belgrade area, J Environ Radioactiv, 79, 297-307, 2005.

16   Tositti, L., Riccio, A., Sandrini, S., Brattich, E., Baldacci, D., Parmeggiani, S., Cristofanelli,

17   P., and Bonasoni, P.: Short-term climatology of PM10 at a high altitude background station

18   in southern Europe, Atmos Environ, 65, 145-152, 2013.

19   Tositti, L., Brattich, E., Cinelli, G., and Baldacci, D.: 12 years of ^{7}Be and ^{210}Pb data in Mt.

20   Cimone, and their correlation with meteorological parameters, Atmos Environ, 87C, 108-

21   122. doi: 10.1016/j.atmosenv.2014.01.014, 2014.

22   Trickl, T., Feldmann, H., Kanter,H.-J., Scheel, H.-E., Sprenger, M., Stohl, A. and Wernli, H.,

23   2010. Forecasted deep stratospheric intrusions over central Europe: case studies and

24   climatologies, Atmos Chem Phys, 10, 499-524.

Atmospheric
Chemistry
and Physics
Discussions

Open Access

EGU

1   Trigo, I.F., Bigg, G.R., and Davies, T.D.: Climatology of cyclogenesis mechanisms in the

2   Mediterranean. Mon Weather Rev, 130, 549-569, 2002.

3   Turekian, K.K., Nozaki, Y., and Benninger, L.K.: Geochemistry of atmospheric radon and

4   radon products. Annu Rev Earth Pl Sc, 5, 227-255, 1977.

5   Turekian, K.K., and Graustein, W.C.: Natural Radionuclides in the Atmosphere, in: Treatise

6   on Geochemistry, Volume 4, Ralph Keeling, F. (Ed.), Holland, H.D., and Turekian, K.K.

7   (executive editors), pp. 347, doi:10.1016/B0-08-043751-6/04042-1, ISBN 0-08-043751-6.

8   Elsevier, p.261-279, 2003.

9   Usoskin, I., and Kovaltsov, G.: Production of cosmogenic [7]Be isotope in the atmosphere: full

10   3D modelling. J Geophys Res, 113, D12107, 2008.

11   van Dingenen, R, Putaud, J.P., Martins-Dos Santos, S., Raes, F. Physical aerosol properties

12   and their relation to air mass origin at Monte Cimone (Italy) during the first MINATROC

13   campaign, Atmos Chem Phys, 5, 2203-2226, 2005.

14   Viezee, W., and Singh, H.B.: The distribution of beryllium-7 in the troposphere. Implications

15   on stratosphere/tropospheric air exchange, Geophys Res Lett, 7, 805-808, 1980.

16   Wilkening, M.H., Clements, W.E., and Stanley, D.: Radon222 flux measurements in widely

17   separated regions, In: The Natural Radiation Environment II, pp. 717-730, U.S. Energy and

18   Res. Dev. Admin., Oak Ridge, Tenn, USA, 1975.

19   Winkler, R., Dietl, F., Frank, G., and Thiersch, J.: Temporal variation of [7]Be and ^{210}Pb size

20   distributions in ambient aerosols, Atmos Environ, 32, 983-991, 1998.

21   WMO-GAW (World Meteorological Organization - Global Atmosphere Watch): 1st

22   International Expert Meeting on Sources and Measurements of Natural Radionuclides

23   Applied to Climate and Air Quality Studies, (Gif-sur-Yvette, France, 3-5 June 2003) (WMO

24   TD   No.   1201),   Report   No.   155   [available   at

Atmospheric
Chemistry
and Physics
Discussions

1   ftp://ftp.wmo.int/Documents/PublicWeb/arep/gaw/gaw155.pdf, last accessed 15 March

2   2016], 2004

3   Zanis, P., Schuepbach, E., Gäggeler, H.W., Huebener, S., and Tobler, L.: Factors controlling

4   Beryllium-7 at Jungfraujoch in Switzerland, Tellus, 51 (4), 789-805, 1999.

5   Zanis, P., Monks, P.S., Schuepbach, R., Carpenter, L.J., Green, T.J., Mills, G.P, Bauguitte, S.,

6   and Penkett, S.A.: In situ ozone production under free tropospheric conditions during

7   FREETEX '98 in the Swiss Alps, J Geophys Res, 105 (D1), 24223-24234, 2000.

8   Zanis, P., Gerasopoulos, E., Priller, A., Schnabel, C., Stohl, A., Zerefos, C., Gäggeler, H.W.,

9   Tobler, L., Kubik, P.W., Kanter, H.J., Scheel, H.E., Luterbacher, J., and Berger, M.: An

10   estimate of the impact of stratosphere-to-troposphere transport (STT) on the lower free

11   tropospheric ozone over the Alps using ^{10}Be and ^{7}Be measurements, J Geophys Res,

12   108(D12), 8520, doi:10.1029/2002JD002604, 2003.

13

14

15

16

17

18

19

20

21

22

23

24

25

1

2

3 **Figures**

4
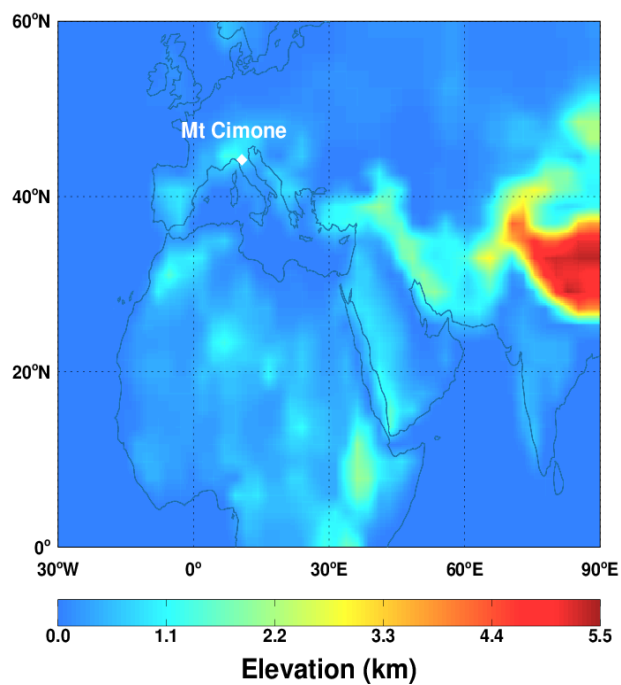
17 **Figure 1.** Surface elevations (km) in the model. The white dot indicates the location of Mt.

18 Cimone (44°12' N, 10°42' E, 2165 m asl).

19

20

21

22

23

1
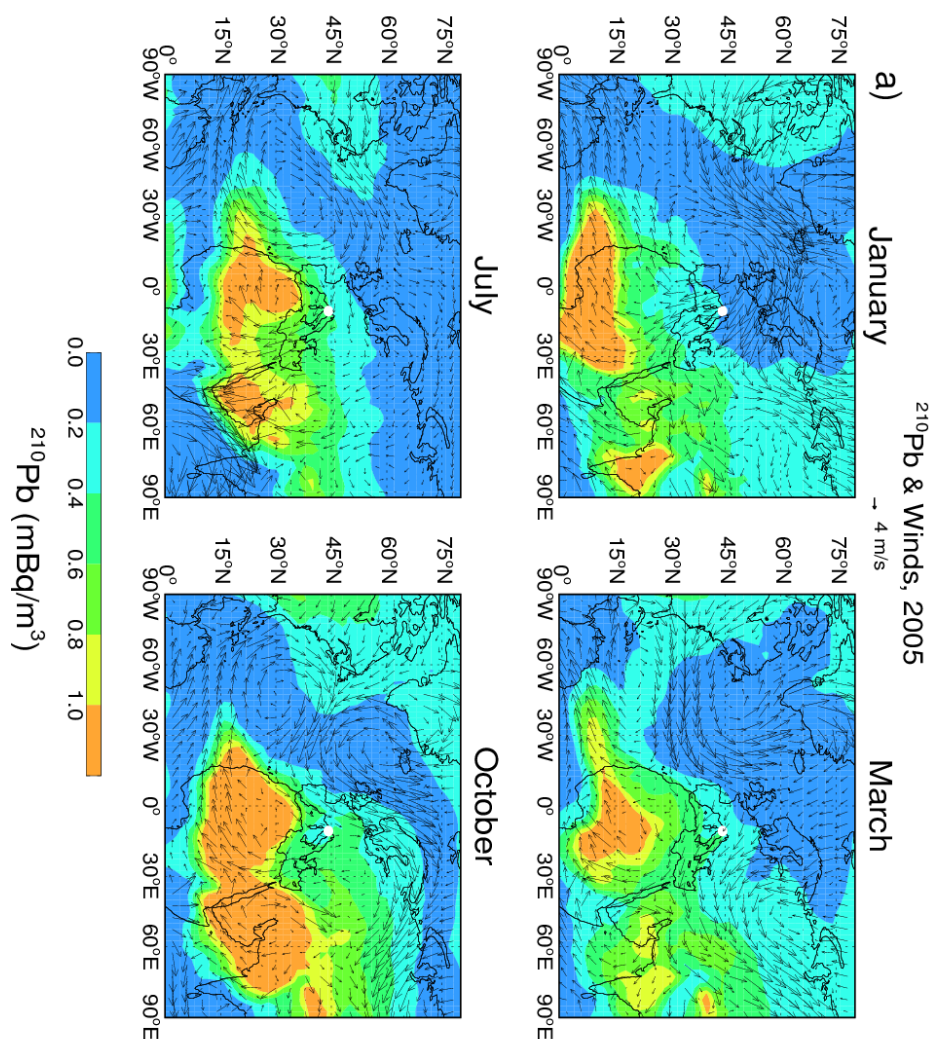
Figure 2. Simulated monthly mean (a) ^{210}Pb concentrations and (b) ^{7}Be concentrations, at the

elevation of Mt. Cimone. Arrows represent the seasonality of winds in the MERRA

meteorological data. The white dot indicates the location of Mt. Cimone (44°12' N, 10°42' E,

2165 m asl). To be continued.
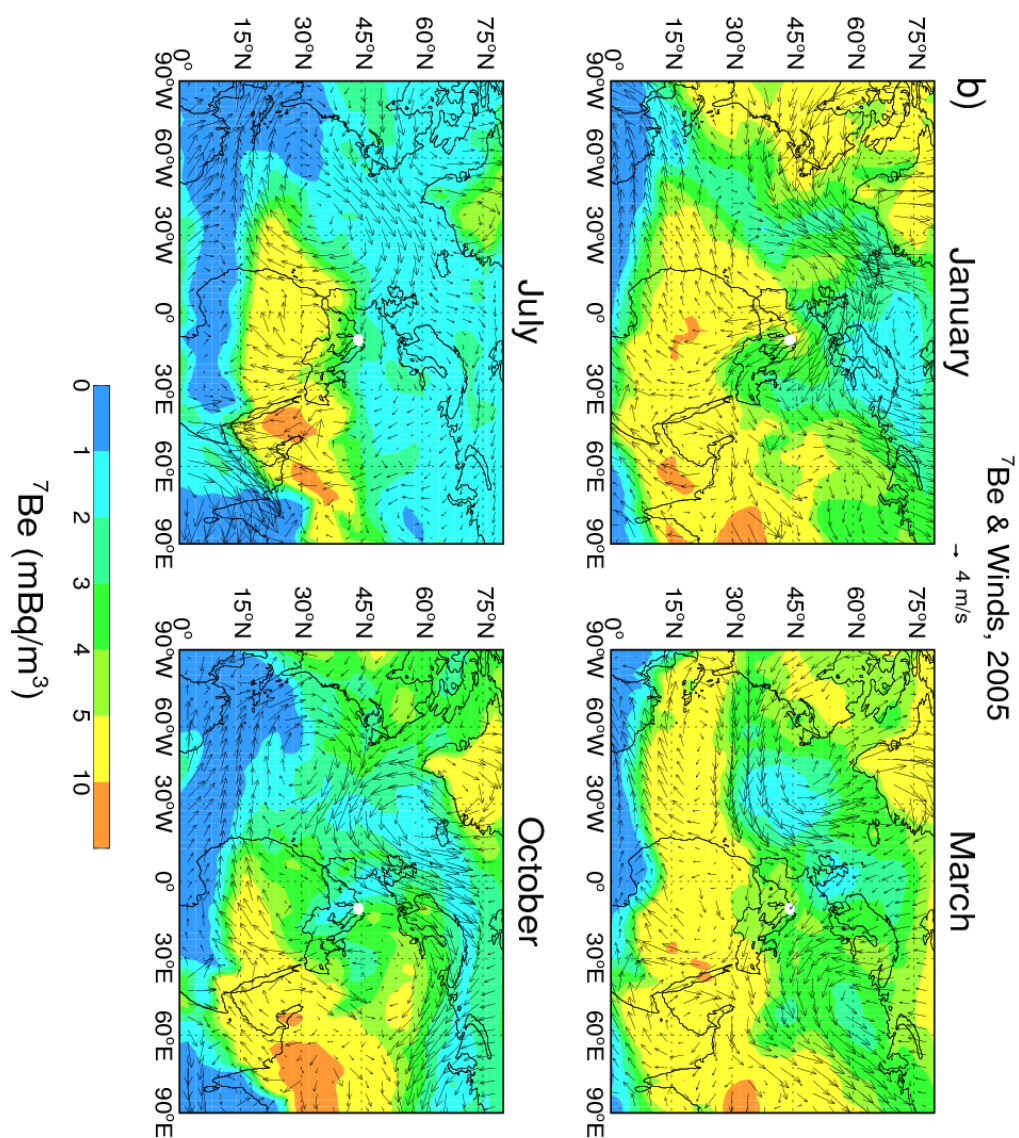
1

2   **Figure 2.** (continued)

3
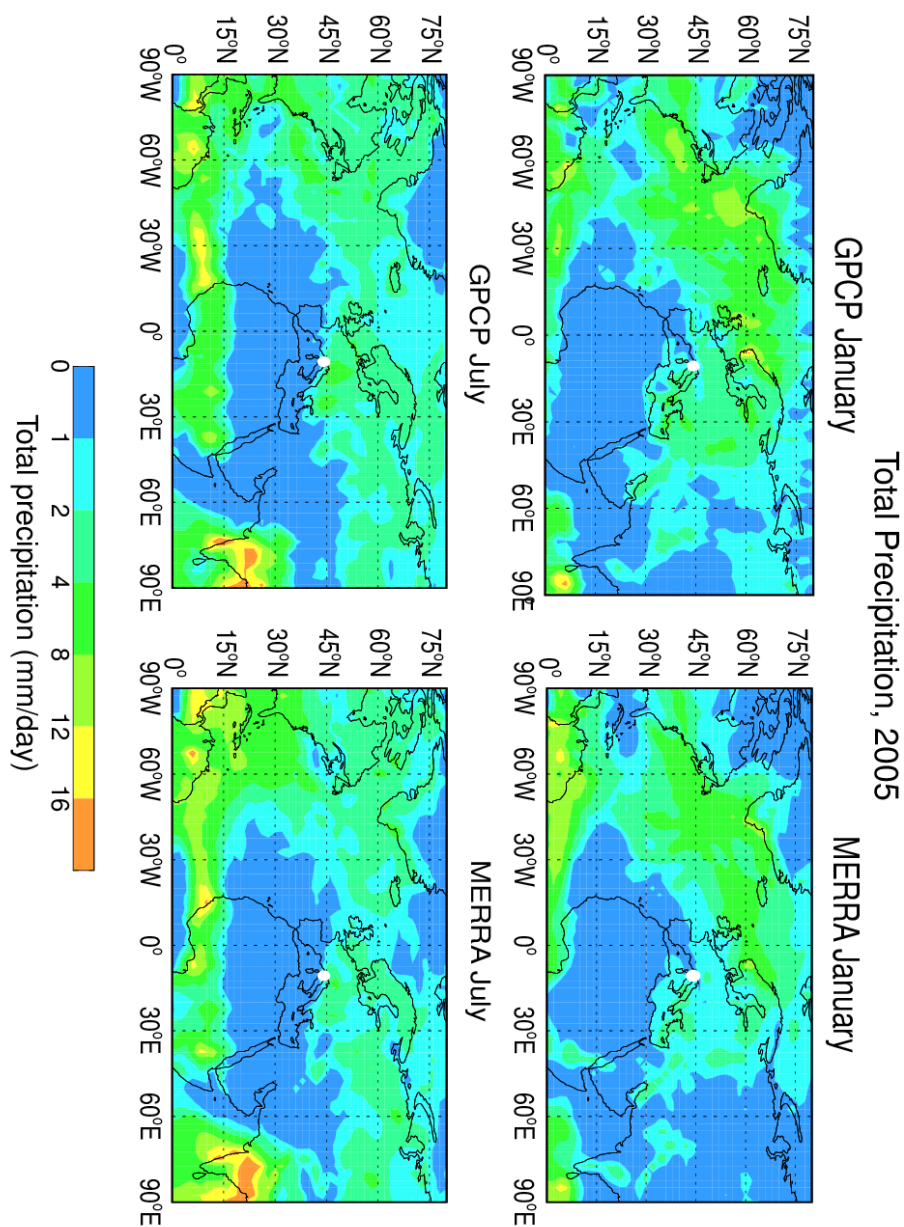
Figure 3. Comparison of the MERRA total precipitation (0-75°N, 90°W-90°E) during January

and July 2005 with that in the GPCP observations. The white dot indicates the location of Mt.

Cimone (44°12'N, 10°42'E, 2165 m asl).
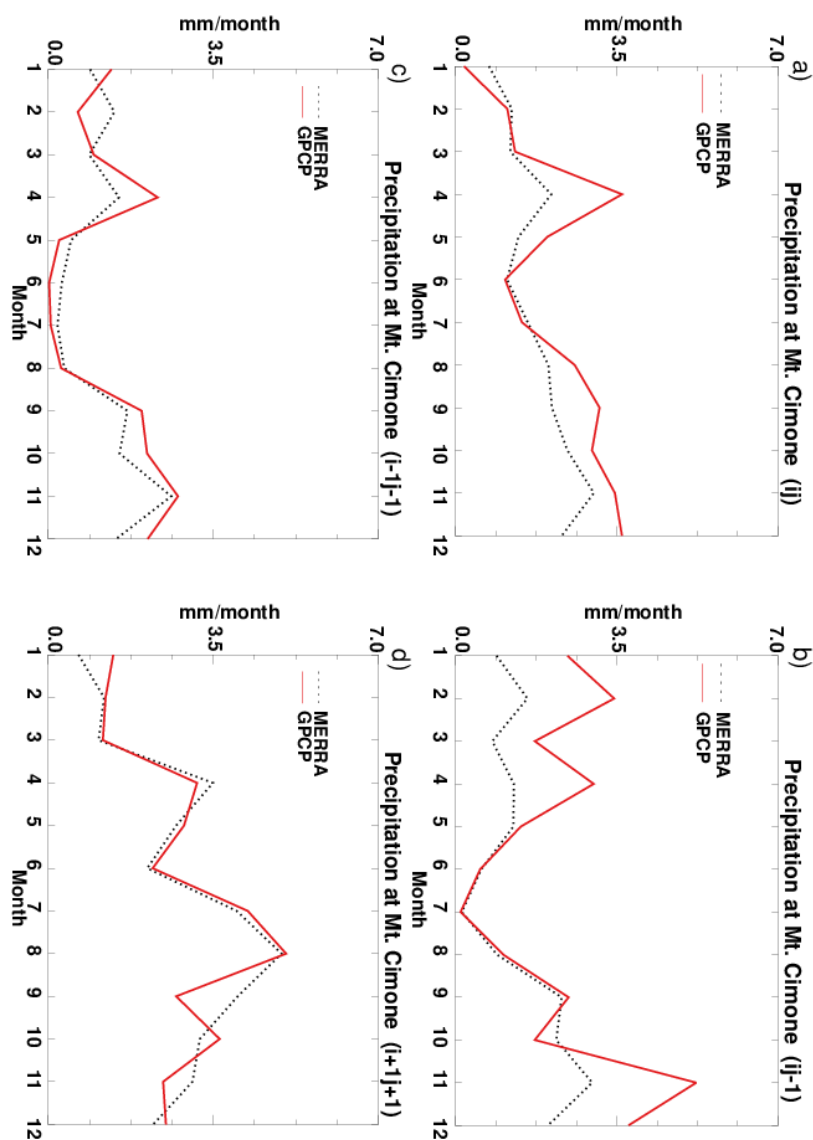
1

2   **Figure 4.** Comparison of the seasonal precipitation at Mt. Cimone in the MERRA

3   meteorological data set with that in the GPCP observations for (a) the model gridbox ("ij")

4   corresponding to the location of Mt. Cimone, (b) the model gridbox ("ij-1") to the west of "ij",

5   (c) the model gridbox ("i-1j-1") to the southwest of "ij", and (d) the model gridbox ("i+1j+1")

6   to the northeast of "ij".

1
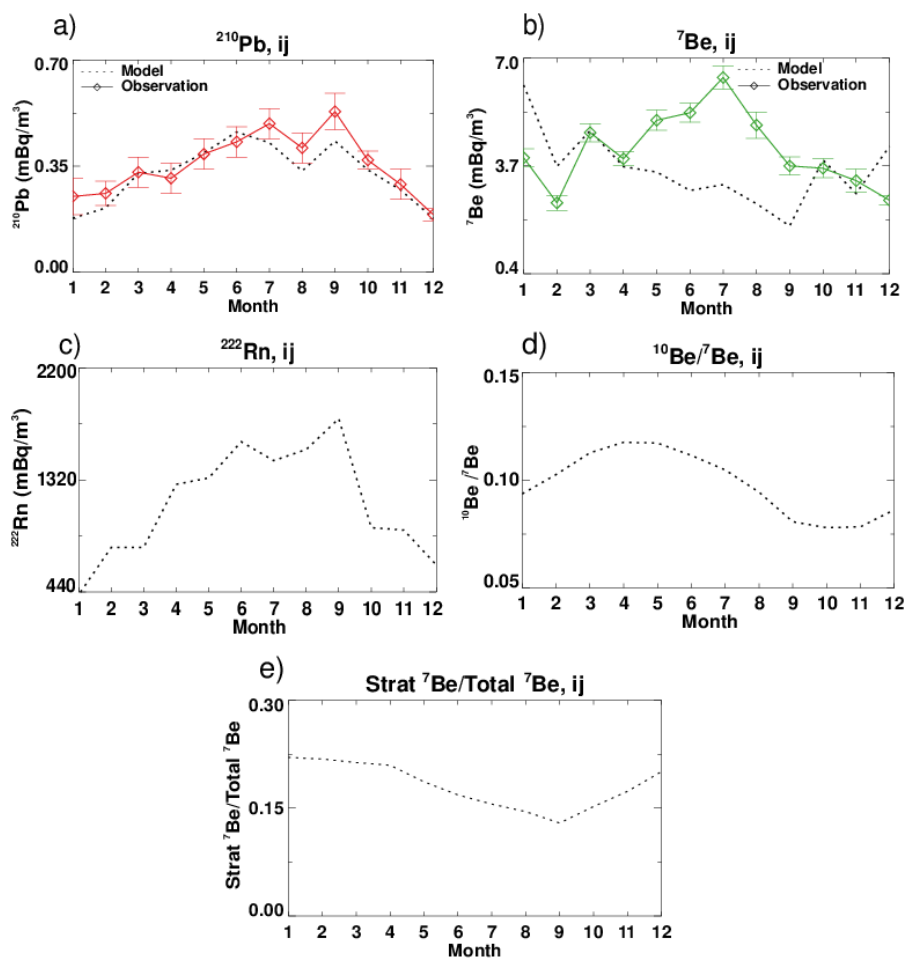
Figure 5 (a,b,c,d,e). Comparison of GMI simulated (black dotted line) monthly (a) ^{210}Pb and

(b) ^{7}Be activities with those observed at Mt. Cimone (solid lines) in 2005. Also shown are GMI

simulated monthly activities of (c) ^{222}Rn, (d) ^{10}Be/^{7}Be ratios, and (e) strat ^{7}Be/total ^{7}Be ratios.

Model values are for the "ij" gridbox corresponding to the location of Mt. Cimone. Vertical

bars indicate the uncertainty in observed activities.
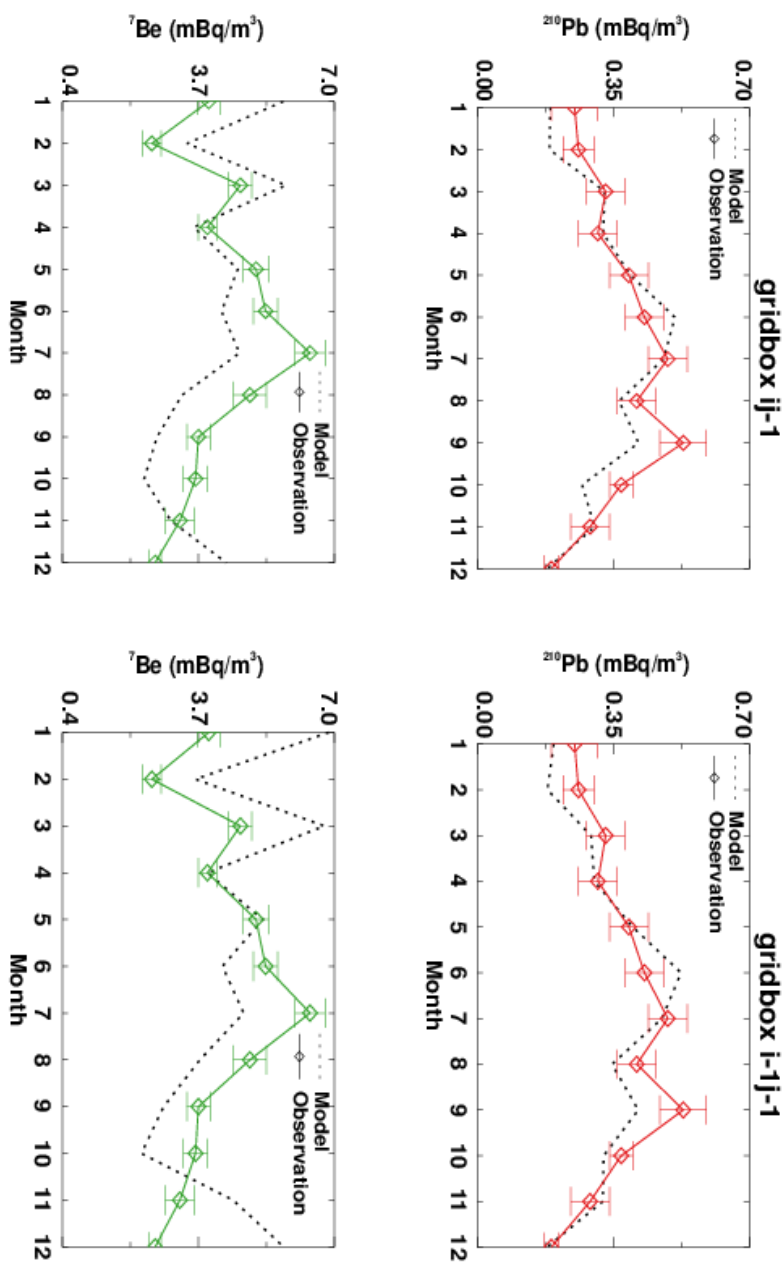
1

2   **Figure 6.** Same as Figure 5(ab), but for the "ij-1" to the south of "ij" (left column) and "i-1j-

3   1" to the southwest of "ij" (right column) grids, respectively.

4

Atmospheric
Chemistry
and Physics
Discussions

1
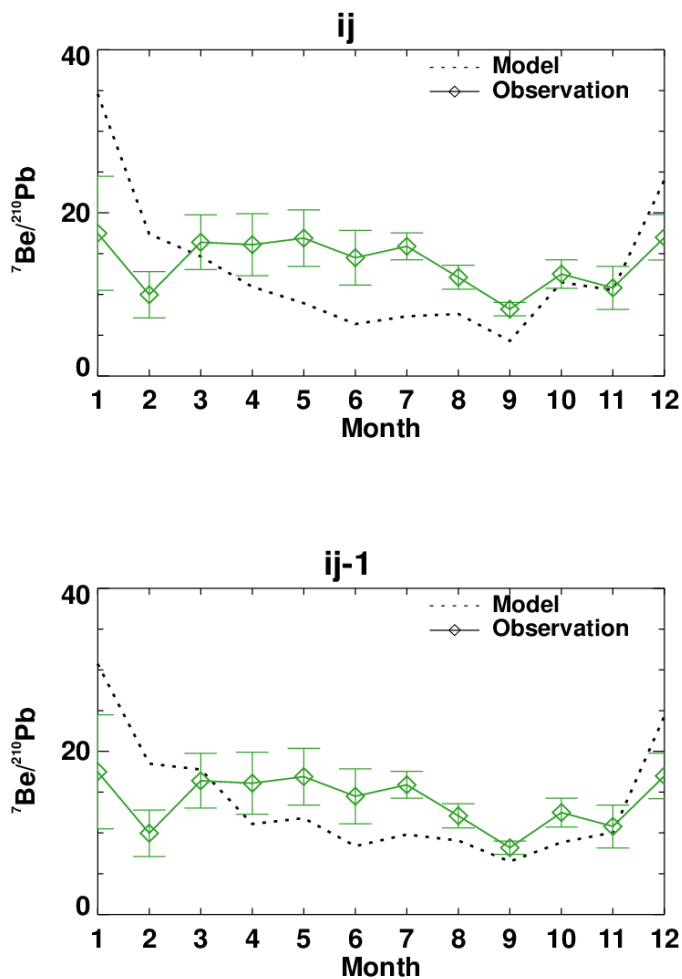
2

3   **Figure 7.** Comparison between GMI simulated monthly ^{7}Be/^{210}Pb ratios at the "ij" and "ij-1"

4   grids (black dotted line) and those from the observations at Mt. Cimone (green solid line).

5   Vertical bars indicate the uncertainty in observed activities.

6

Atmospheric
Chemistry
and Physics
Discussions
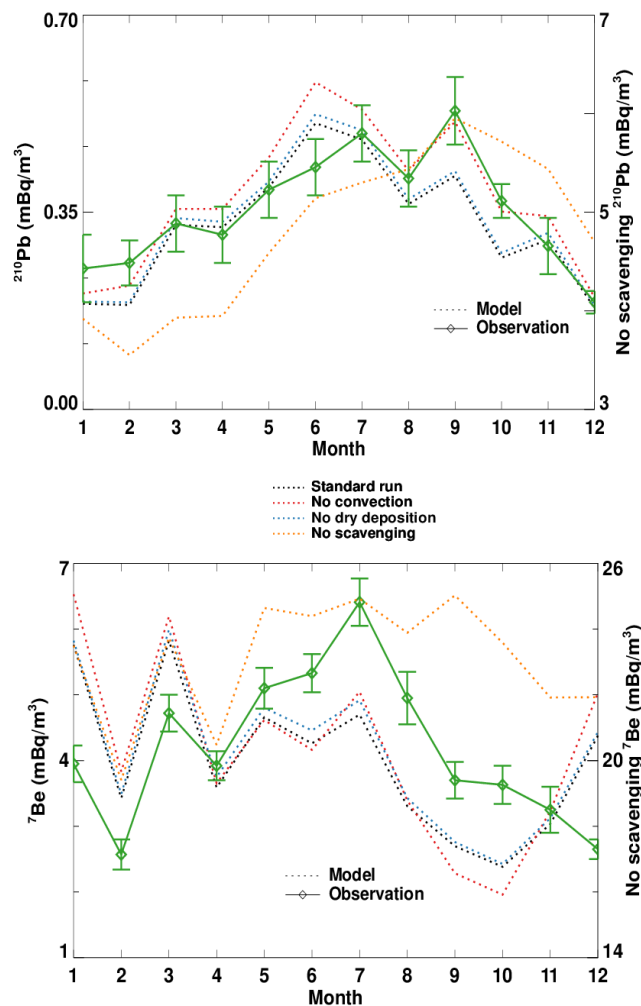
Figure 8. Comparison of GMI simulated monthly ^{210}Pb and ^{7}Be activities at Mt. Cimone

between the standard (black dotted line) and the sensitivity runs ("ij-1" grid). The sensitivity

runs are those without convective transport/scavenging (red dotted line), without dry deposition

(blue dotted line), and without scavenging (orange dotted line; y-axis on the right). The

observations are shown as green solid line. Vertical bars indicate the uncertainty in observed
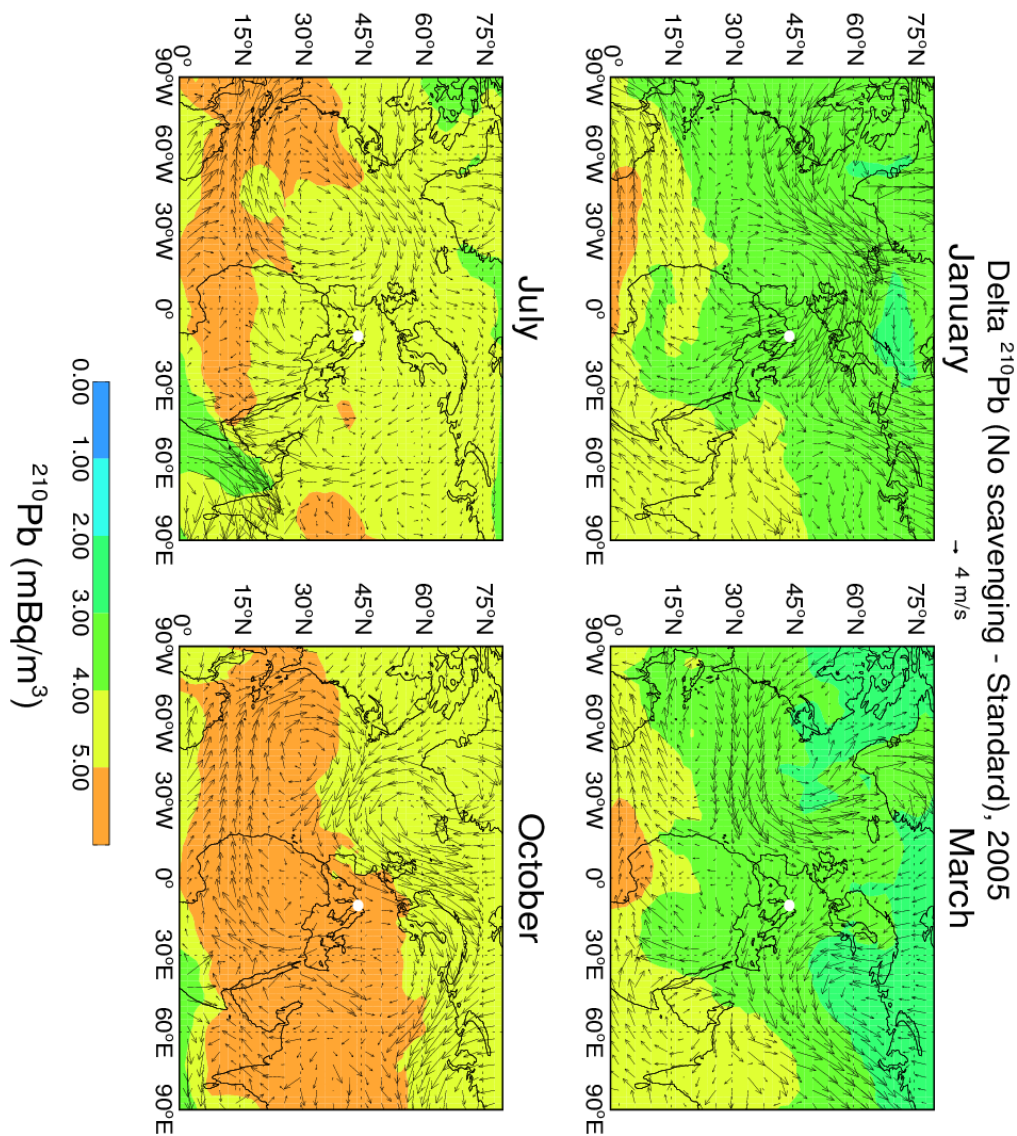
activities.

1

2
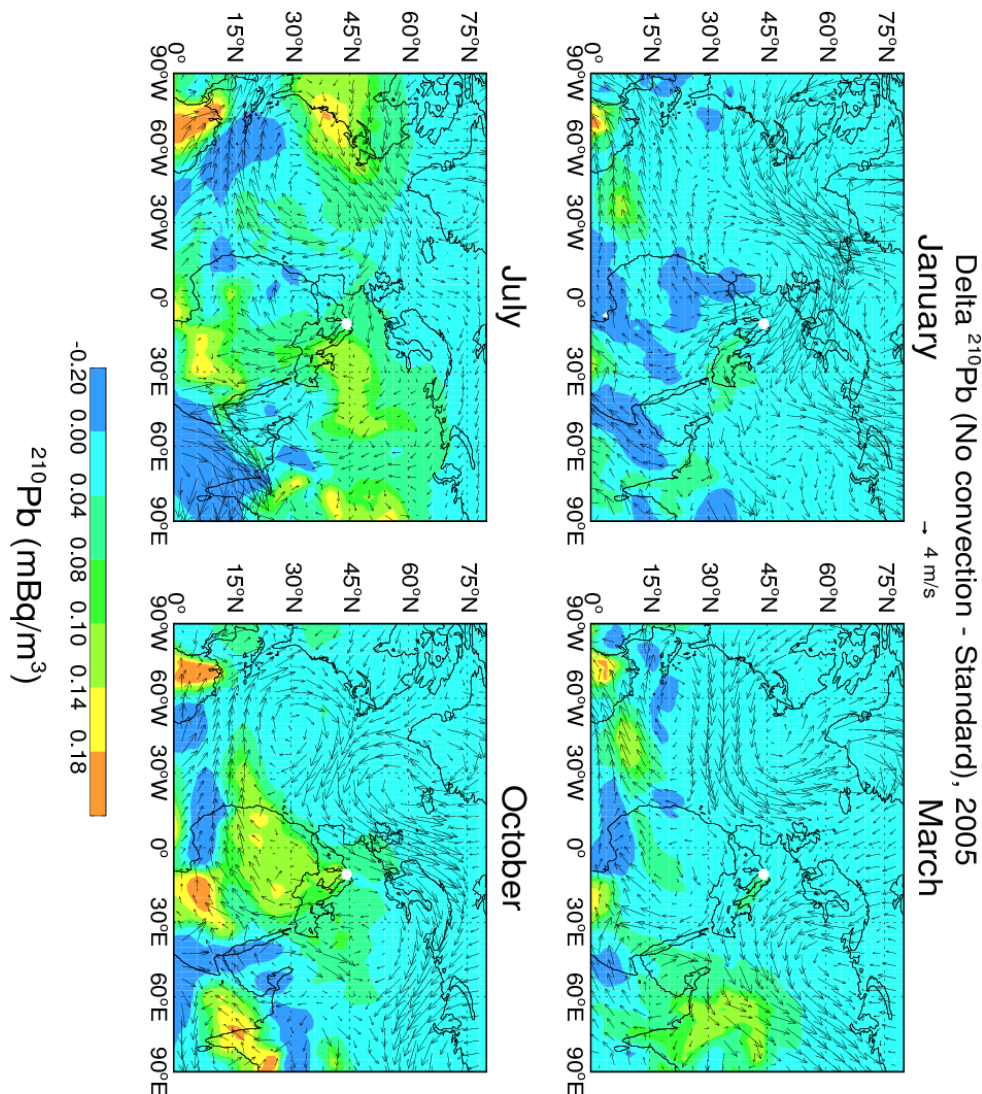
Figure 9. GMI simulated differences of ^{210}Pb concentrations at the elevation of Mt. Cimone

between a sensitivity run without convection (i.e., without transport and scavenging in

convective updrafts) and the standard run. Arrows denote MERRA winds. The white dot

indicates the location of Mt. Cimone (44°12' N, 10°42' E, 2165 m asl).
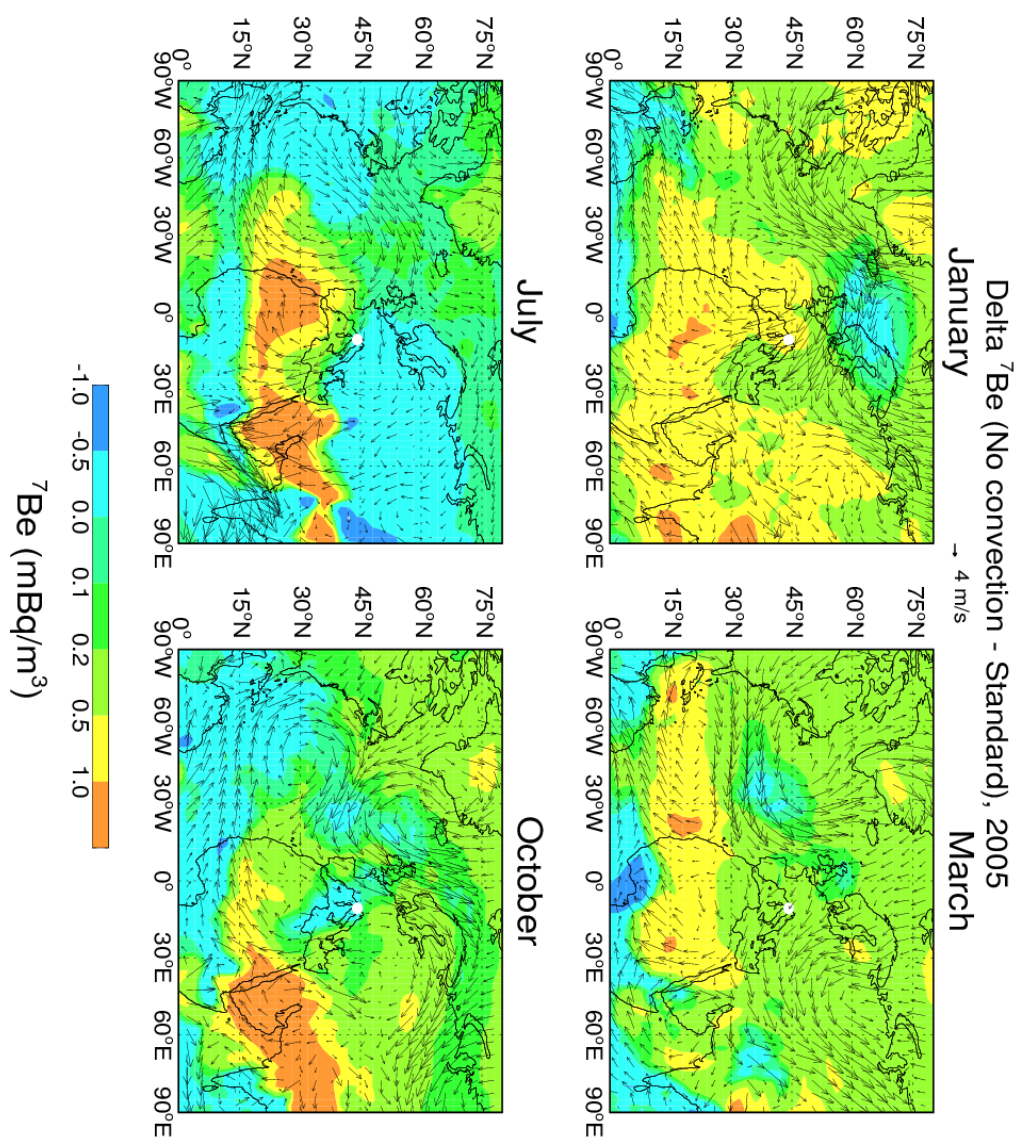
Atmospheric
Chemistry
and Physics
Discussions

1

2

3 **Figure 10.** Same as Figure 9, but for a sensitivity simulation where wet scavenging is turned

4 off.

5
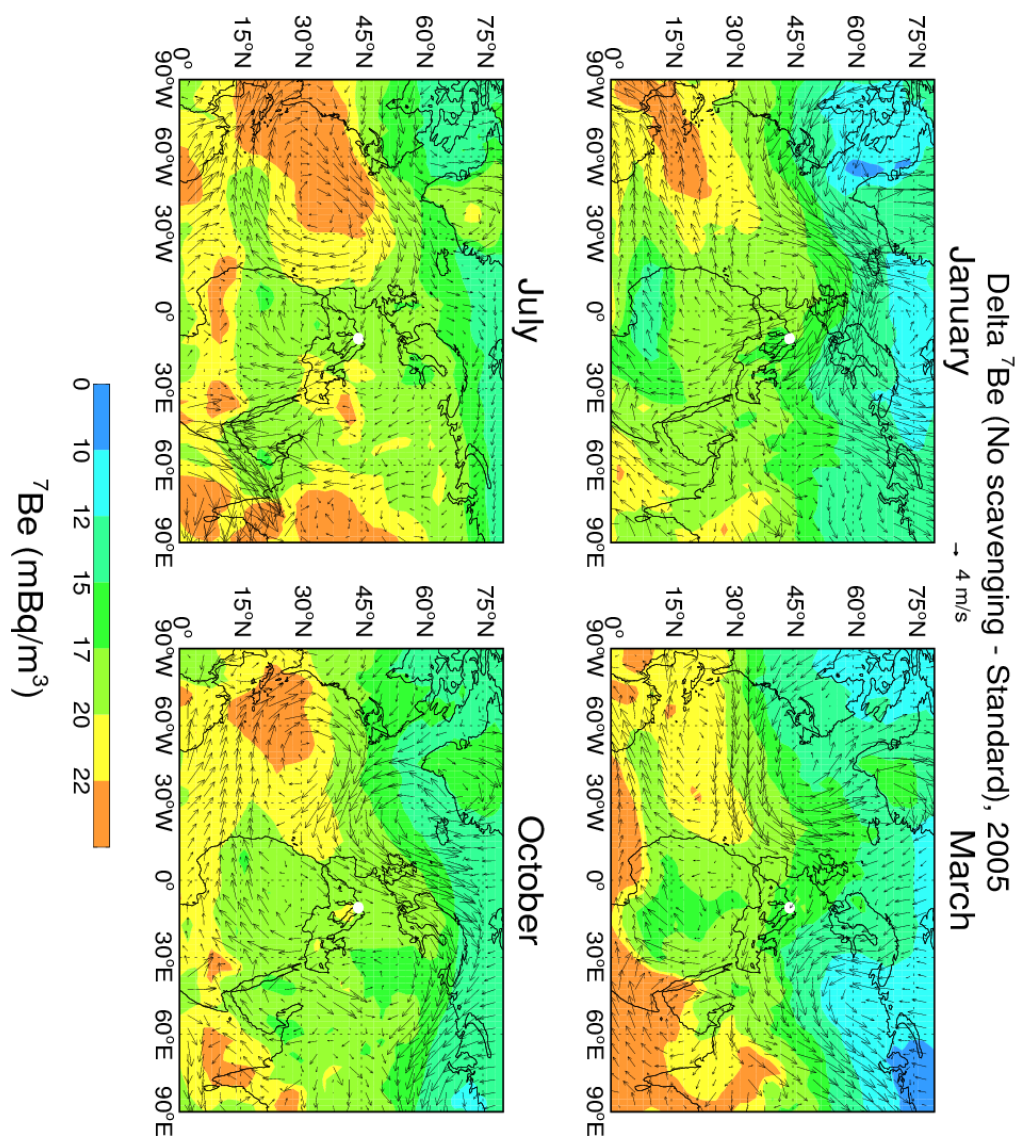
1

Figure 11. GMI simulated differences of ⁷Be concentrations at the elevation of Mt. Cimone

between a sensitivity run without convection and the standard run. Arrows denote MERRA

winds. The white dot indicates the location of Mt. Cimone (44°12' N, 10°42' E, 2165 m asl).

5

1

2

Figure 12. Same as Figure 11 but for the difference between a sensitivity run without wet

scavenging and the standard run.

5